

Characterization of Heterogeneity Style and Permeability Structure in Fluvial Reservoirs

by

Mark Barton, Edward Angle, and Joseph Yeh

Bureau of Economic Geology

and

Benjamim N. Carrasco

PETROBRÁS

Final report prepared for PETROBRÁS under contract no. 6502032931

Bureau of Economic Geology
Noel Tyler, Director
The University of Texas at Austin
Austin, Texas 78713-8924

July 1995

CONTENTS

ABSTRACT	1
INTRODUCTION	2
GEOLOGIC SETTING/BACKGROUND	3
METHODS AND DATA	7
Outcrop Characterization	7
Stratigraphic Geocellular Modeling of Reservoir Attributes	9
LOCATION OF STUDY SITE (KM 99)	10
TERMINOLOGY AND ANALYSIS	11
DESCRIPTION OF STRATA	12
Mudstone-dominated Body	13
Fine-grained Heterolithic Facies	13
Erosive-based Sandstone Body	13
INTERPRETATION OF DATA	23
PERMEABILITY CHARACTERISTICS AND STRUCTURE	29
Permeability Characteristics	31
Permeability Structure	33
Spatial Correlation of Permeability	35
STRATAMODEL GEOCELLULAR PERMEABILITY MODEL	37
CONCLUSIONS	39
ACKNOWLEDGMENTS	40
REFERENCES	40

Figures

1. Maps showing distribution of Cretaceous strata in the Potiguar Basin and locations of study area and vertical logs and permeability transects..... 5
2. Gamma-ray log showing characteristics of correlation units, Açu Formation 6

3a. Cross section showing sedimentological logs, paleocurrents, and distribution of stratal surfaces, Km 99	14
3b. Cross section showing distribution of architectural elements, Km 99	16
3c. Cross section showing distribution of permeability profiles and grain size classes, Km 99	18
4. Photograph of transverse bar facies eroding into abandoned channel-fill facies (hand on contact) from section D8	22
5. Photograph of transverse bar facies from section D18	24
6. Channel-belt evolution of storey sets i, ii, and iii	26
7. Plane view of facies architecture for storey sets i, ii, and iii	27
8. Probability plot of permeability versus grain size	32
9. Probability plot of permeability for architectural elements	32
10. Semivariogram of permeability for pebbly coarse-grained and medium-grained sandstone	37
11. Semivariogram of permeability for erosive-based sandstone body	37

Table

1. Permeability characteristics of sandstone body architectural elements	30
--------------------------------------------------------------------------------	----

Foldouts (in envelope)

Stratamodel sequences

Stratamodel permeability

Diskette (3-inch PC format, in envelope): Permeability data, Açu outcrop study, Km 99

ABSTRACT

The Cretaceous Açu Formation was investigated as an analog to a heterogeneous group of reservoirs having significant potential for reserve growth in the Potiguar Basin of Brazil. Architectural, lithologic, and petrophysical information was collected from an outcrop exposing a fluvially deposited sandstone body located in the state of Rio Grande do Norte, Brazil. Sedimentologic descriptions of the sandstone body were collected from a series of vertical transects spaced evenly across the outcrop. Stratal surfaces traced between transects were recorded on photomosaics. Measurements of permeability were obtained from each transect by use of a portable probe-style mechanical field permeameter. A cross section depicting bedding architecture, sedimentologic attributes, and permeability values was constructed and the information incorporated into a two-dimensional representation of reservoir architecture using Stratamodel's Stratigraphic Geocellular Modeling software (SGM). The SGM technique deterministically interpolates permeability data between transect locations using a lithologic or stratigraphic framework.

The outcrop examined exposes a 10-m-thick, 300-m-wide sandstone body along a two-dimensional cross section subparallel to the depositional axis. Architecturally, the sandstone body is composed of multiple truncating channel storeys that display vertically stacked and sidelapping relationships. Storeys are defined by a basal erosion surface overlain by an intraformational mud-clast breccia. Individual storeys range in thickness from 1 to 5 m and extend in length from 20 to 240 m. Within channel storeys, component bedsets generally steepen (channel bar) then progressively decrease in dip from the concordant to discordant storey margin (channel fill). Individual bedsets range in thickness from 0.2 to 2 m and may be as long as 100 m. Channel-bar deposits are characterized by a uniform to upward-coarsening, medium-grained to very coarse grained, pebbly to granular sandstone sequence that passes laterally into channel-fill deposits characterized by a uniform to upward-fining, massive to trough cross-stratified coarse-grained

sandstone sequence. Component bedsets also coarsen upward and display large-scale avalanche foreset bedding as much as 2 m thick. Foresets dip as much as 33 degrees, are tangential to the underlying surface, and are transitional with a thin-bedded, medium- to coarse-grained, horizontally stratified sandstone or pebbly mudstone. The sandstone body is interpreted to record the superposition of a series of alternate bars within a low- to moderate-sinuosity channel by downstream rather than lateral channel migration. The fact that channel-fill deposits are nearly as coarse as channel-bar deposits indicates that channel segments were not rapidly abandoned; instead, filling must have been associated with a gradual diversion of discharge into an adjacent channel.

Grain size is the dominant control on permeability. Other factors that are of importance are sorting and the presence of ductile mud clasts. A visual comparison of permeability profiles and stratal architecture indicates (1) permeabilities are reduced one to three orders of magnitude near bedset and channel-storey bounding surfaces; (2) channel-bar deposits and component bedsets are characterized by consistent upward-increasing permeability trends; and (3) adjacent channel-fill deposits are characterized by reduced permeabilities that display an erratic to upward-decreasing trend.

INTRODUCTION

Oil and gas reservoirs typically display a complex architecture that fundamentally controls paths of fluid migration, recovery efficiency, and ultimately, the volume of hydrocarbons left in a reservoir at the time of abandonment. Improved recovery efficiency, particularly in mature reservoirs, requires an advanced understanding of reservoir anatomy (i.e., the spatial distribution of the properties that affect fluid flow). With a detailed understanding of how reservoir fabric develops and controls fluid flow paths, drilling strategies can be designed and implemented that more efficiently target remaining, conventionally recoverable hydrocarbons that are prevented from migrating to the wellbore by intrareservoir seals or bounding surfaces. Outcrop characterization of reservoir facies is one means for understanding heterogeneity in sedimentary deposits.

Characterization from outcrops allows for the continuous sampling necessary for a detailed reservoir description that is not available from subsurface data alone.

In an effort to understand the architecture of depositional and diagenetic facies and their relationship to petrophysical attributes that directly control fluid and steam flow in the reservoir, an exposure of the Cretaceous Açu Formation was investigated as an analog to a heterogeneous group of reservoirs having significant potential for reserve growth. An outcrop of the Açu Formation was selected because of the importance of remaining resources in this reservoir type in the Potiguar Basin of Brazil. Low recovery efficiencies in this hydrocarbon play, which range from 9 to 42 percent, indicate that substantial reserves remain and highlight the potential for incremental recovery through accurate reservoir characterization.

The predictability of reservoir properties composes the crux of this report, which addresses the spatial distribution of permeability in fluvial sandstones. The approach used in this investigation was to establish the depositional architecture of a fluvially deposited sandstone body and determine what factors affect the spatial distribution of permeability. Sedimentological, stratigraphic, and petrophysical data were collected from the outcrop and incorporated into a two-dimensional representation of reservoir architecture using Stratamodel's Stratigraphic Geocellular Modeling (SGM) software. The end product is a quantitative image of internal reservoir structure. Results from this study may be used to address the effects of heterogeneities on recovery efficiency and the sensitivity of recovery predictions to uncertainty descriptions and to identify controls on recovery in order to focus further data collection and descriptions for site-specific studies.

GEOLOGIC SETTING/BACKGROUND

The Potiguar Basin is located in the onshore and shallow offshore portions of northeastern Brazil and occupies an area of 40,000 km². The basin is dominated by a series of northeast-southwest half-grabens that originated during Early Cretaceous time as the African and South American continental plates separated from each other. The basin is underlain by basement crystalline rocks (Precambrian) that encompass a north-to-northeastward-thickening wedge of

sedimentary rocks (Cretaceous) that is crossed by narrow bands of alluvial sediments associated with modern incised fluvial systems (fig. 1a).

The Cretaceous sedimentary section consists of the basal Açu Formation, the overlying Jandaira Formation, and the Ponta do Mel Formation. The Açu Formation is an Albian to Cenomanian clastic unit that ranges in thickness from 250 to 700 m and consists of an upward-fining cycle of mudstones, siltstones, sandstones, and conglomerates. The sandy character of the Açu Formation and the absence of regional stratigraphic markers and poor biostratigraphic resolution make correlation difficult. However, on the basis of electric logs from 400 exploratory wells, the formation has been informally divided into four lithostratigraphic "correlation units" (Vasconcelos and others, 1990), designated from the base up as Açu 1, Açu 2, Açu 3, and Açu 4 (fig. 2). The basal unit (Açu 1), is relatively thin, generally less than 100 m, and discontinuous, but where present it consists of coarse clastics representative of a system of alluvial fans and fluvial channels. Overlying the Açu 1 interval are two upward-fining successions referred to as Açu 2 and Açu 3, respectively. Each upward-fining succession shows, from the base to the top, a transition from highly interconnected coarse-grained sandstone bodies to isolated coarse- to medium-grained sandstone bodies encased in fine-grained sediments. Each interval has been interpreted to represent a system of braided to meandering channels and associated environments. The Açu 4 interval consists of an upward-fining succession of fine-grained sandstones and shales that range in thickness from 50 to 150 m. Açu 4 deposits are interpreted to represent a coastal estuarine and deltaic system. The fine sandstones and shales that cap the Açu Formation grade upward into shallow-marine mudstones, limestones, and dolomites of the Jandaira Formation, making a transgressive sequence. Laterally, the coarse clastics of the Açu Formation grade offshore to fine-grained clastics and limestones of the Ponta do Mel Formation, which are believed to have been deposited in a shelf setting.

The Açu Formation contains important hydrocarbon reservoirs within the Potiguar Basin. Depth of production is relatively shallow, with most oil fields found at depths of between 500 and 1500 m. Oil traps are mainly structural and related to basement highs (Castro and others, 1981).

(a)

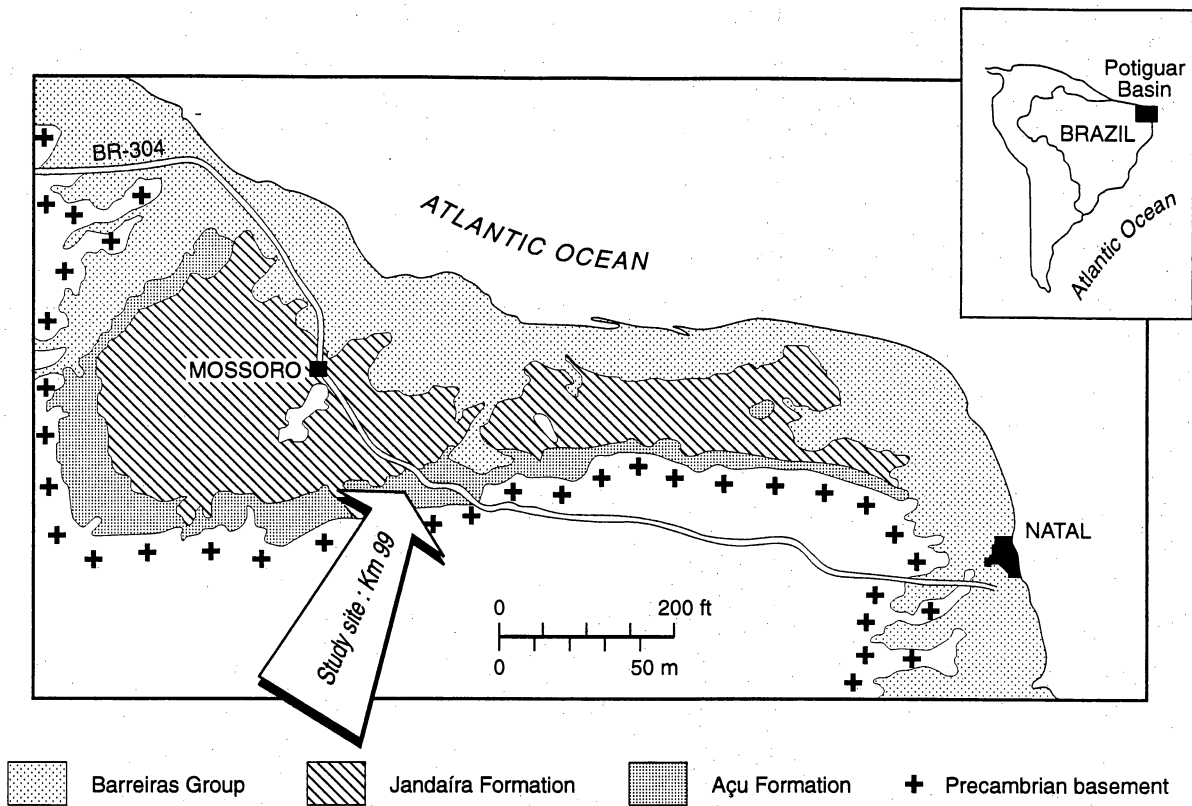
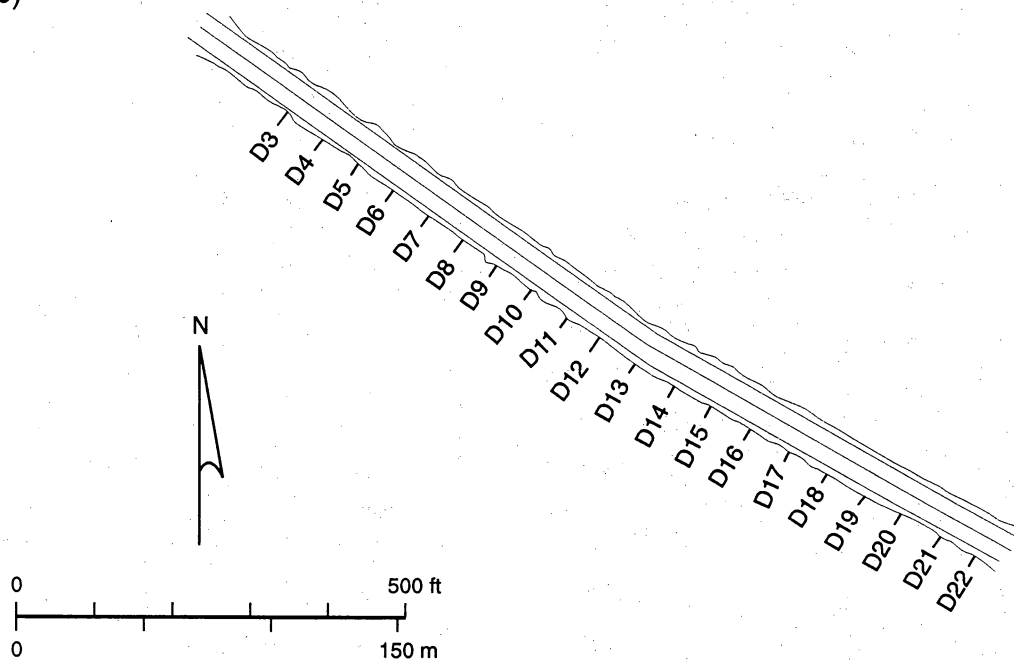


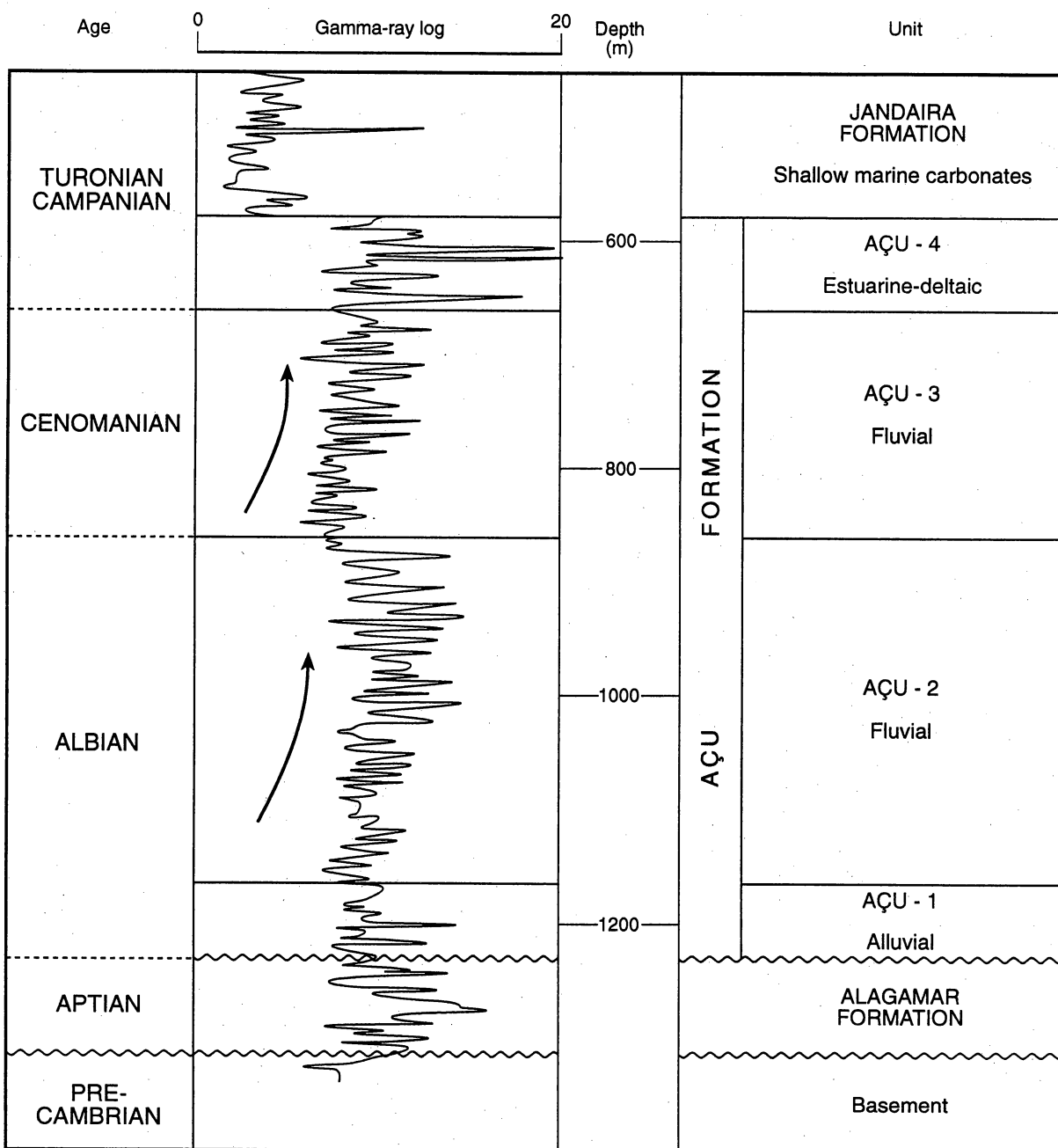
Figure 1a. Map showing distribution of Cretaceous strata in the Potiguar Basin and location of study area.

(b)



QAb352c

Figure 1b. Map showing location of vertical logs and permeability transects.



Adapted from Vasconcelos and others (1990)

QAb353c

Figure 2. Gamma-ray log showing characteristics of correlation units, Açu Formation.

Production is largely (approximately 70 percent) from the fluvially deposited section of the Açu Formation; one oil field produces from the estuarine-deltaic section. Despite relatively high permeabilities that in places exceed a darcy, estimated recoveries within the fluvially deposited reservoirs are relatively low, ranging from 9 to 42 percent.

METHODS AND DATA

This project was conducted by a joint team of Bureau of Economic Geology, The University of Texas at Austin and Petrobras CENPES personnel. Three principal tasks were involved (1) calibration of the Petrobras minipermeameter, (2) outcrop characterization of a sandstone body of special interest to Petrobras, and (3) spatial modeling of permeability by use of Stratamodel's SGM. Task 1 was completed in August 1994, and results are detailed by Carrasco (1994). The results of tasks 2 and 3 are the focus of this report, as summarized below.

Outcrop Characterization

Steps involved in the outcrop characterization included mapping of facies architecture and quantification of permeability variation. Information gathered on the outcrop was assembled into a cross section depicting bedding architecture, distribution of principal lithofacies, and measured permeability values for each vertical transect.

Sedimentologic descriptions of the sandstone body were collected from a series of vertical transects spaced evenly across the outcrop. Sedimentologic data collected included lithology, grain size, sorting, sedimentary structures, intensity of burrowing, presence and type of lithologic discontinuities, and paleoflow orientations. Stratal surfaces were traced between transects and recorded on photomosaics that provided complete coverage of the outcrop.

Measurements of permeability were obtained directly from the outcrop by use of a portable probe-style mechanical field permeameter (minipermeameter). Previous work by Goggin and others (1988) has demonstrated the minipermeameter to be an excellent field device for detailed

sampling of large outcrops. The minipermeameter is a simple gas-flow device that measures a given gas-flow rate at a specified pressure drop. Gas (nitrogen) from a compressed source, a 20-L portable bottle, is passed through the minipermeameter and into the rock from an injection tip. The flow rate is then monitored by a series of rotameters, each of which consists of a float and flow tube. To calculate permeability, a modified version of Darcy's law reported by Goggin and others (1988) is utilized. The minimum and maximum detection limits of the minipermeameter used in this investigation are approximately 0.1 md and 10,000 md, respectively. Prior to testing, weathered material was removed from the sample site, and a clean flat surface capable of maintaining a non-leaky seal between the injection tip and the rock surface prepared. Weathered material was removed from the sample site with a hand-held core plugger. A clean flat surface was prepared within the core hole by chipping away small rock fragments with a hammer and chisel. The chisel was never directly applied to the sample site in order to avoid inducing fractures.

Data collected at the outcrop were recorded in a spreadsheet format (Microsoft Excel) and sent to Petrobras-CENPES-DIGER in care of Dr. Claudio Bettini on June 18, 1994. For each sample site, the data set consists of a vertical position in meters relative to the top of the outcrop, a horizontal position relative to transect no. 22, permeability measurement in millidarcys, and a description of geologic attributes that include grain size, sedimentary structures, lithofacies, and facies association. This stratigraphic, depositional, and lithologic information provides the basis for establishing discrete permeability groups on the basis of lithofacies relations and documenting the relationship of permeability structure to stratigraphic architecture. By comparing sedimentary attributes with permeability values, the influence of depositional and diagenetic processes on sandstone heterogeneity is evaluated and the factors that most significantly control permeability variation can be determined.

Two methods were used to examine the permeability structure. One method involves the correlation of permeability profiles and the other the application of the statistical semivariogram technique. Both methods estimate the lateral and vertical continuity of zones with similar permeabilities. In the first method, bounding surfaces subdivide the reservoir analogue into

constituent lithofacies and lithofacies assemblages from which permeability patterns and characteristics are interpreted and mapped in detail. A visual assessment of permeability patterns is established by comparing adjacent profiles and tracing sets of strata from one locality to another along the outcrop (Stalkup and Ebanks, 1986). This comparison allows the sampled area to be divided into subintervals with different levels of permeability. The subintervals represent permeability classes having a finite lateral and vertical continuity along the exposure. By measuring the continuity of different subintervals, an estimate of the correlation of zones with similar permeability is developed.

In the second method the spatial correlation of permeability is estimated by the semivariogram function. The semivariogram function expresses the average similarity between spatially separated pairs of measurements. The function can be used to populate the space between limited data sets with petrophysical attributes such as permeability. The semivariogram function assumes that the data are normally distributed and stationary. A power transformation (p-normal), used by Jensen and others (1987), has been used to render a given data set normally distributed prior to semivariogram analysis.

Stratigraphic Geocellular Modeling of Reservoir Attributes

Stratamodel geocellular modeling of the data was conducted following the fieldwork at Bureau of Economic Geology facilities in Austin, Texas. Using Stratamodel's Stratigraphic Geocellular Modeling (SGM) software, stratigraphic, sedimentologic, and petrophysical data collected at the outcrop were incorporated into a two-dimensional representation of permeability structure within the reservoir analog. The SGM technique preserves geologic reality by deterministically correlating permeability data within a lithologic and/or stratigraphic framework.

LOCATION OF STUDY SITE (KM 99)

An outcrop of special interest to Petrobras (considered a representative example of a fluvially deposited reservoir facies within this region) was selected for investigation, and sedimentologic and petrophysical data from the outcrop were collected during March and April 1994. The study site is located along the southern margin of the Potiguar Basin in the state of Rio Grande do Norte, Brazil (fig. 1a). Exposures in this region are generally poor and limited to a few widely spaced outcrops and roadcuts. Descriptions of the geology of nearby outcrops are provided by Cordeiro de Farias and others (1990). A previous study, conducted by Becker and other (1992), investigated the geometric attributes of lithologic units exposed at the study site. Açú outcrops in this area have been correlated with the lithostratigraphic Açú 3 unit in the subsurface (Becker and others, 1992).

The section is exposed along the northeast face of the roadcut located between Km 99 and 100 on highway BR 304. The exposure is about 350 m long. Strata dip into the subsurface at the southeast end of the roadcut and have been removed by erosion at the northwest end. A map view of the roadcut with the position of vertical transects where geologic and permeability data were collected is shown in figure 1b. Sedimentologic and petrophysical data were collected from the exposure along a series of evenly spaced transects that were 15 to 20 m apart. Permeability measurements were made with a portable mechanical field permeameter (minipermeameter) at 0.1-m intervals along each vertical transect. A total of 926 measurements from 20 vertical transects were collected. In addition, permeability measurements were collected at 1-m spacings from a 320-m horizontal transect that spanned the total lateral distance between vertical transects. Along this transect, data were also collected at 0.1-m spacing in three intervals that ranged from 5 to 7 m in length. In total, more than 1,400 outcrop permeability measurements were obtained.

TERMINOLOGY AND ANALYSIS

The outcrop was subdivided with respect to bounding surfaces and lithofacies. Lithofacies describe portions of the rock with common characteristics and are named after their dominant physical attribute. Lithofacies are important because they define sets of variables such as texture and mineralogy that influence permeability. Textural differences (grain size) were used as the main criteria for subdividing the outcrop into lithofacies groups. Textural differences are useful because (1) they display a close relationship to permeability, (2) they are a relatively simple measure to quantify, (3) they can be related to electric log facies, and (4) they are an attribute portable to depositionally similar subsurface settings.

Bounding surfaces are erosional as well as nondepositional discontinuities that based on cross-cutting relationships subdivide the reservoir analog into a hierarchy of bedding elements. Bedding elements are useful because they describe common associations of lithofacies that range in scale from individual sets of strata to an entire channel fill complex (Allen, 1963; Friend, 1983, Jackson, 1975; Miall, 1985, 1988a, 1988b). Three orders of bounding surfaces were considered in this investigation; from smallest to largest, this hierarchy consists of bedsets, storeys, and storey sets. Bedsets are equivalent to lateral accretions of Allen (1983), and stratum bounded by third-order surfaces of Miall (1988a) and are composed of a conformable succession of lithofacies deposited during a depositional event. An example would be a single epsilon cross bed. Beds within sets are strata containing similar lithofacies or are associated with individual sedimentary structures and are equivalent to first and second-order surfaces of Miall (1988a). Storeys are defined at their base by a major erosion surface and are internally composed of a set of inclined beds. Each channel storey normally consists of a set of inclined bedsets that dip in a single direction such that they concordantly overlies one storey margin (channel bar) and are discordant with the opposite storey margin (channel fill). An example would be a point bar deposit composed of a succession of epsilon cross beds. Storey sets are defined at their base by a major erosion surface and define groups of genetically related channel storeys.

Subsequent interpretations of sandstone body architecture are detailed by Willis (1993) and based on the following attributes: (1) alignment of stories within a sandstone body; (2) truncation relationships between adjacent storeys; (3) lateral changes in bedset inclination and steepness within each storey; (4) changes in grain size and sedimentary structures within each storey; (5) paleocurrent orientations relative to bedset dip trends across individual storeys; and (6) changes in paleocurrent orientations between adjacent stories. Alongstrike variations in these attributes reflect (1) temporal and spatial variations of bar geometry and facies, (2) bar migration and channel cutoff, which controls facies preservation, and (3) the outcrop orientation. The storey records channel incision and subsequent bar formation and migration. The stacking pattern of storeys reflect the changes in the channel through time due to channel migration and cutoff. Component bedsets represent deposits of individual flood events. Bedset set thickness reflects distances the bar and channel migrated during individual depositional events. Alongstrike variation of bedsets within stories record changes in the channel bed through time due to bar growth and migration.

DESCRIPTION OF STRATA

The outcrop examined exposes a 7-m-thick, 300-m-wide erosive based sandstone body bounded by crudely bedded, red mottled mudstones and heterolithic, thinly bedded, fined-grained sandstones and siltstones. A series of two-dimensional cross sections, subparallel to the depositional axis of the sandstone body, were constructed (fig. 3a–3c). Cross section 3a provides sedimentological logs, paleocurrent measurements, and the distribution of stratal surfaces. Cross section 3b shows the distribution of architectural elements exposed within the outcrop, including channel bar, channel fill, fine-grained channel fill, thin-bedded heterolithic deposits, and the mudstone-dominated deposits. Cross section 3c shows bar graphs (permeability profiles) of permeability measurements taken from the vertical transects and distribution of grain size classes.

Mudstone-dominated Body

The sandstone body is bounded by massive to crudely bedded, red mottled mudstones and siltstones. The basal contact of the sandstone body with the mudstones is erosional, whereas the upper contact is abrupt but conformable. The mudstones are disrupted by rootlets and burrows and contain carbonate in the form of nodules and tubules. Laterally, the mudstone-dominated facies beneath the erosional contact interfinger with thinly bedded, fine-grained sandstones and siltstones. The limited lateral extent and poor exposure of the mudstone-dominated facies precludes accurately determining the thickness and lateral extent of this element.

Fine-grained Heterolithic Facies

The fine-grained, thin-bedded heterolithic facies consists of a succession of decimeter- to centimeter-thick bedsets with flat bases that progressively thin in the direction of paleoflow and fine upward. Paleocurrents are directed to the east and southeast, approximately normal to the northeast to northwest paleocurrents in the erosive-based sandstone body. The coarsest bedsets are dominated by small to medium cross-stratification, whereas finer grained bedsets are dominated by parallel and ripple cross stratification. Sediment disruption in the form of burrowing and root casts causes poor preservation of current structures, especially in the upper and distal portion of the deposit. Locally, small dune bedforms with internal planar cross stratification are completely preserved. In the direction of paleocurrents, bedsets gradually fine, thin, become increasingly disrupted, and divide into multiple beds.

Erosive-based Sandstone Body

The sandstone body consists predominantly of coarse to pebbly coarse-grained sandstone with minor amounts of conglomerate, medium- to fine-grained sandstone, and rare siltstone and mudstone. In the sandstone classification of McBride (1963), the Açu sandstones are arkosic to

(a) Bedding diagram and lithologic descriptions

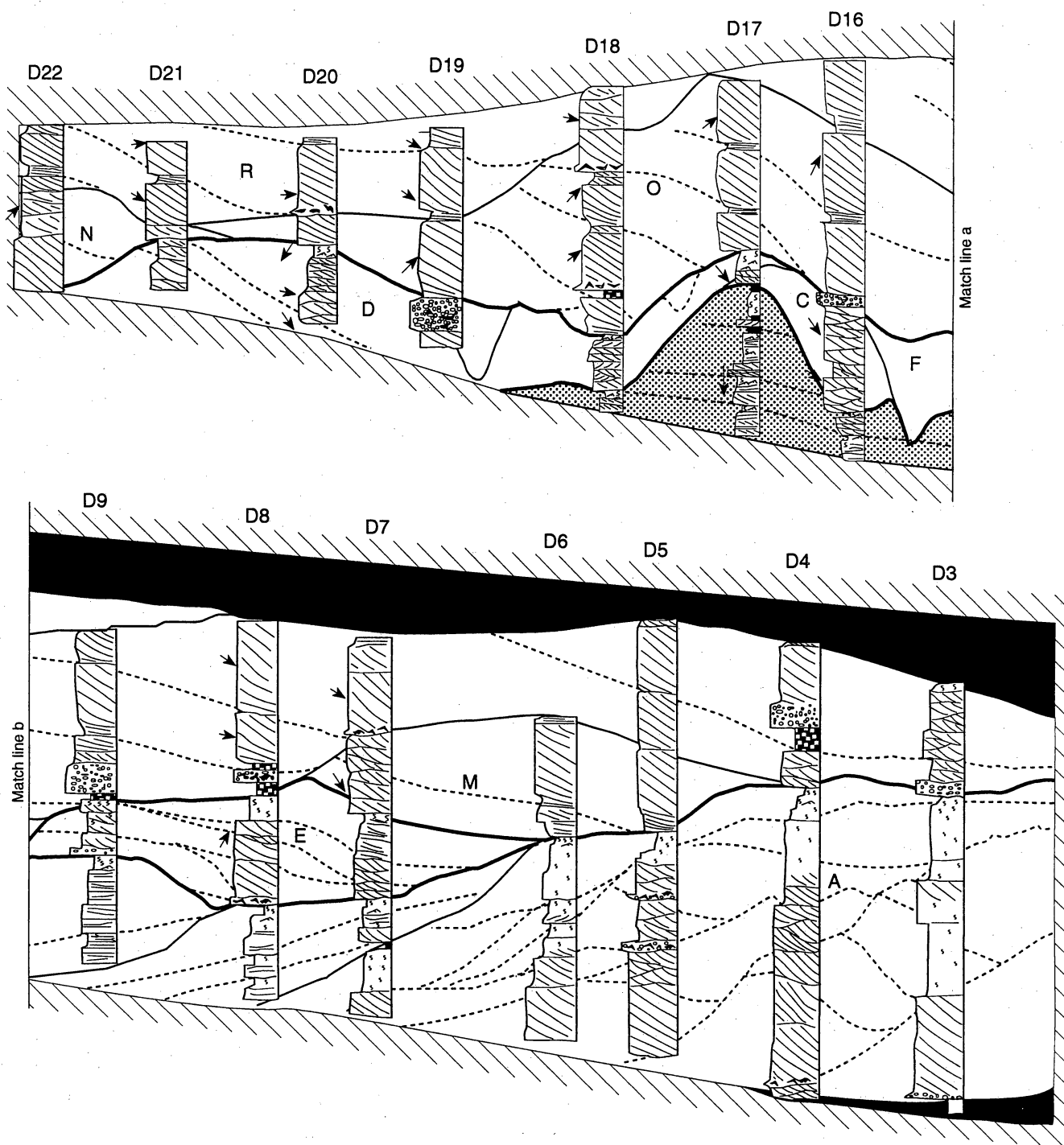


Figure 3a. Cross section showing sedimentological logs, paleocurrents, and distribution of stratal surfaces, Km 99.

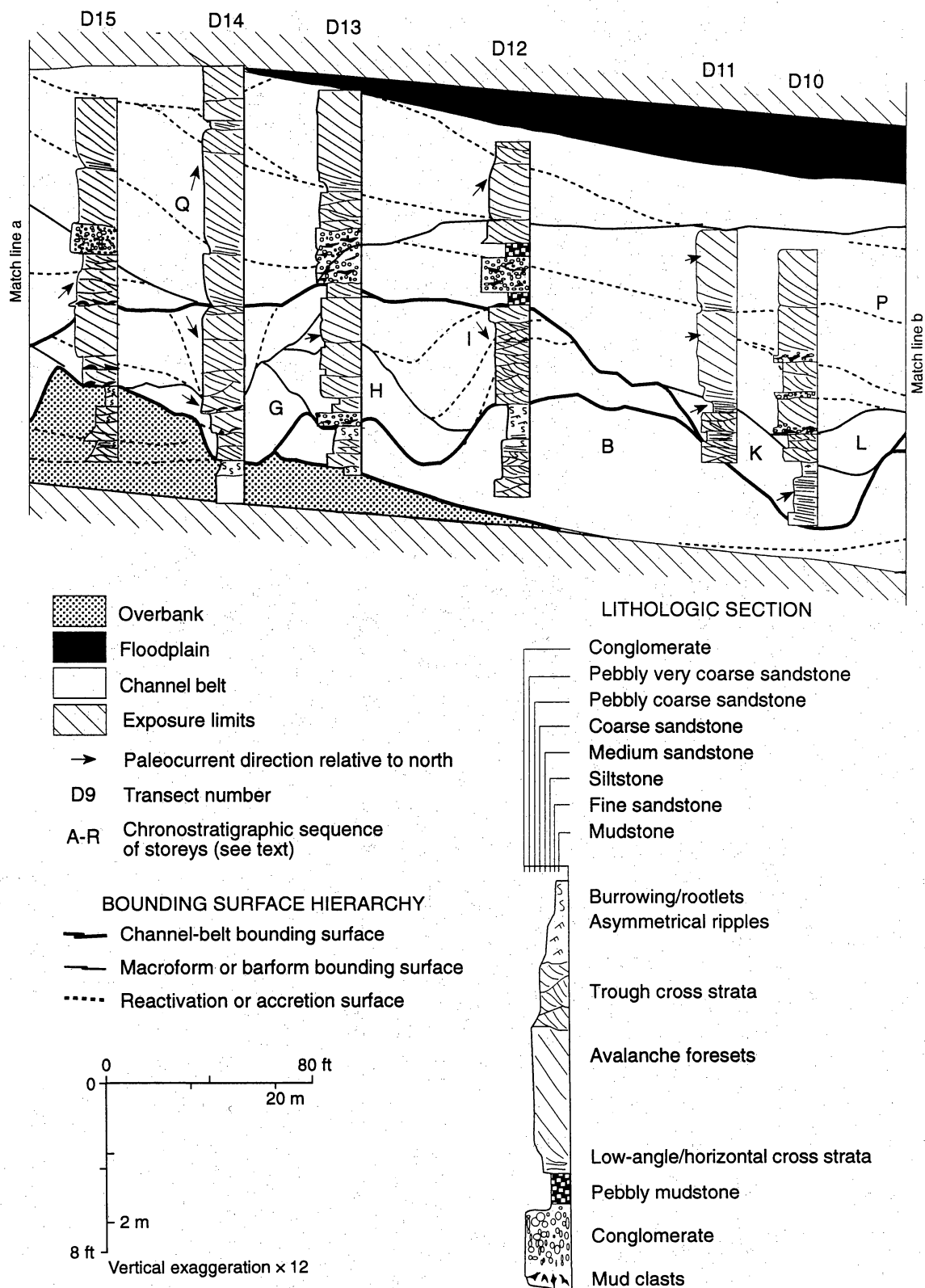


Figure 3a (continued)

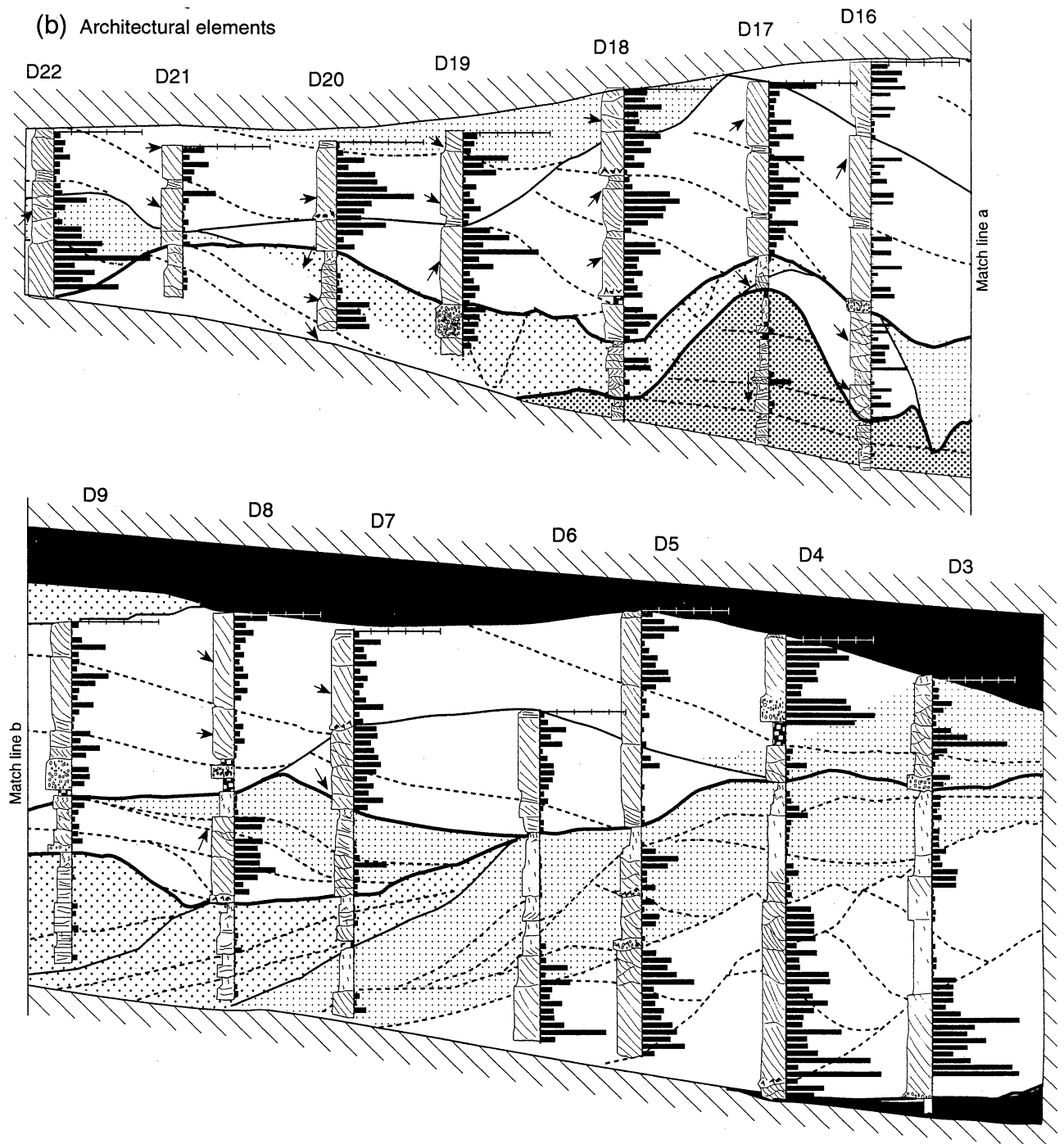


Figure 3b. Cross section showing distribution of architectural elements, Km 99.

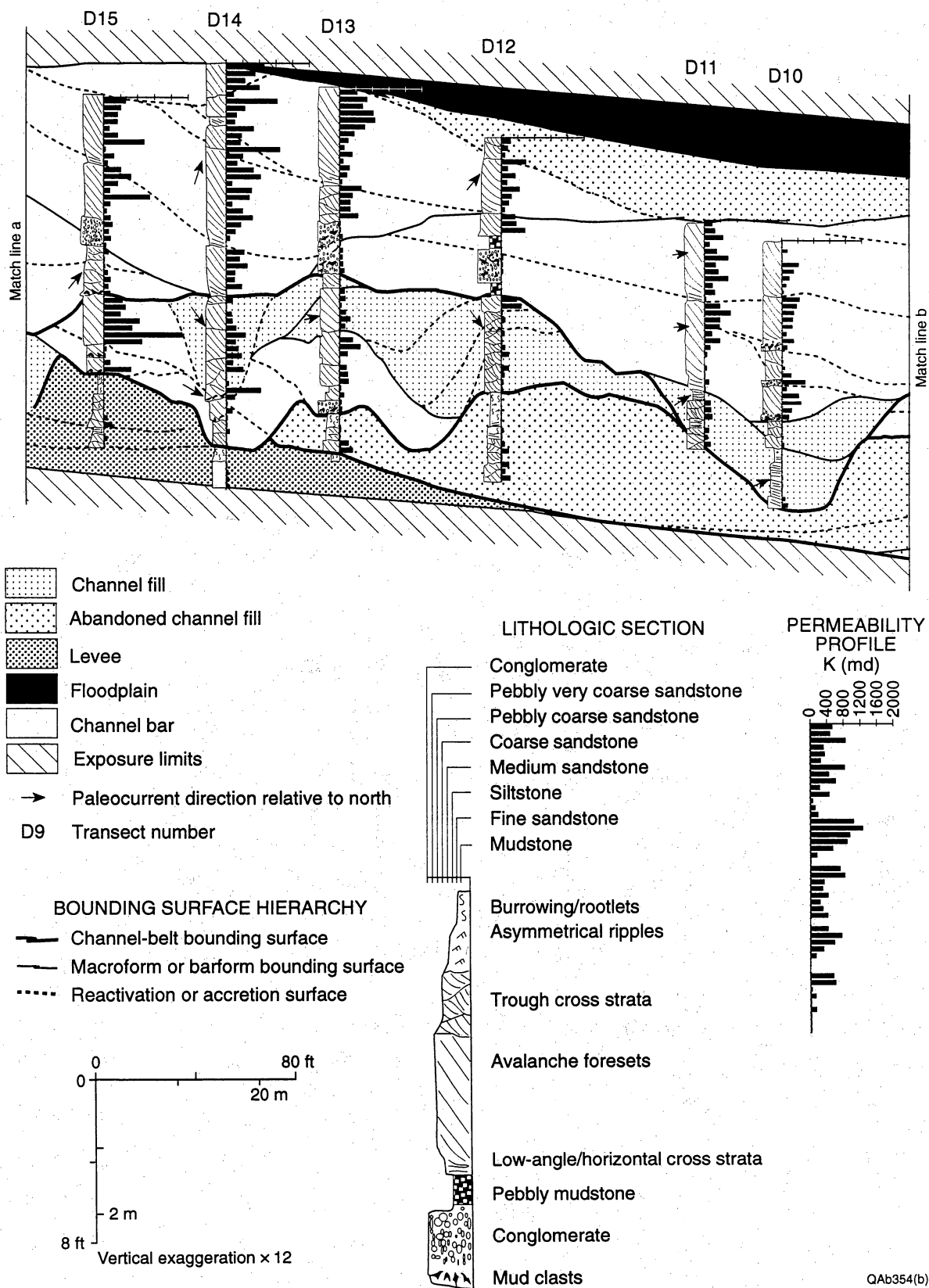


Figure 3b (continued)

(c) Permeability profiles and distribution of grain-size groups

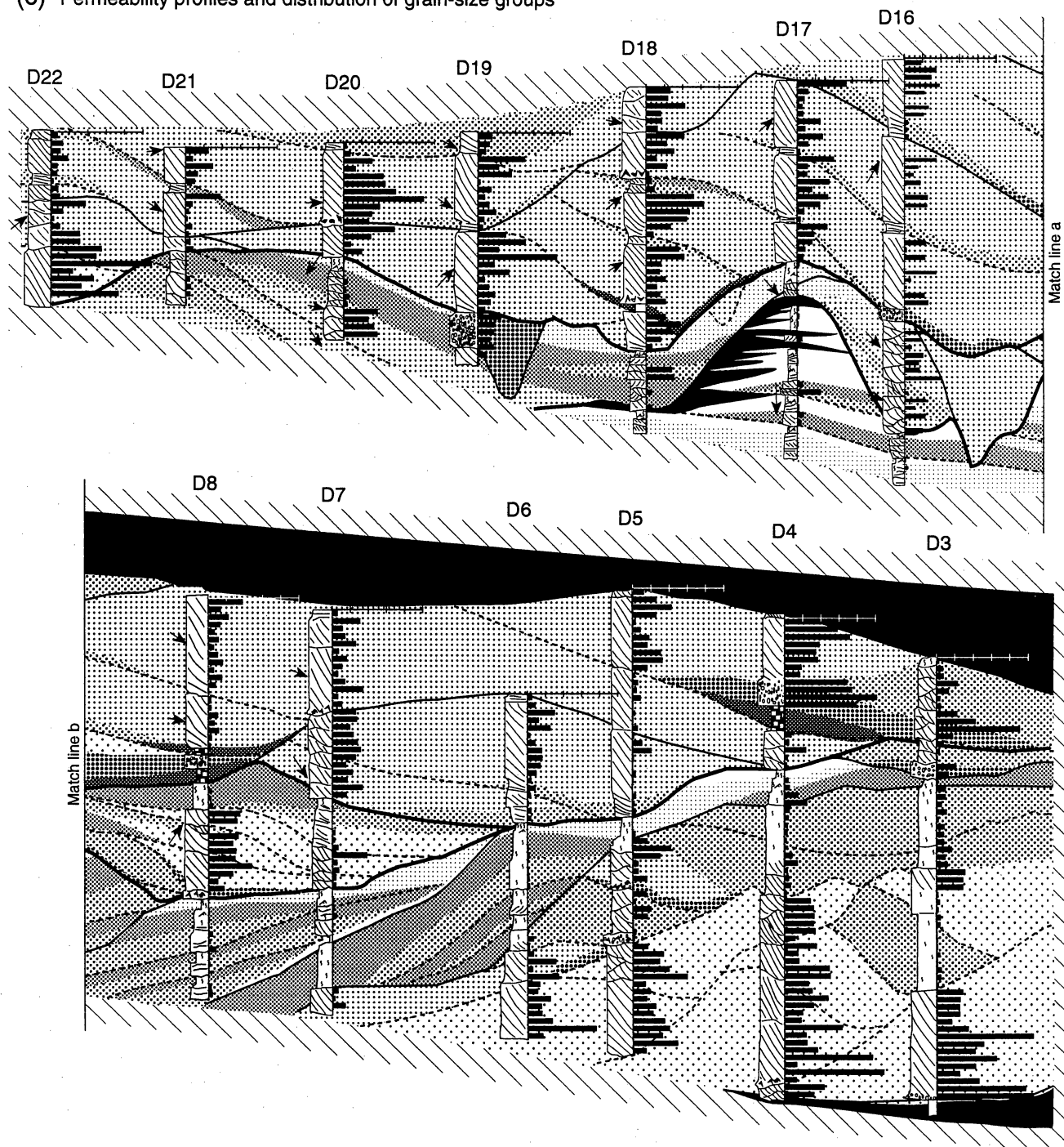
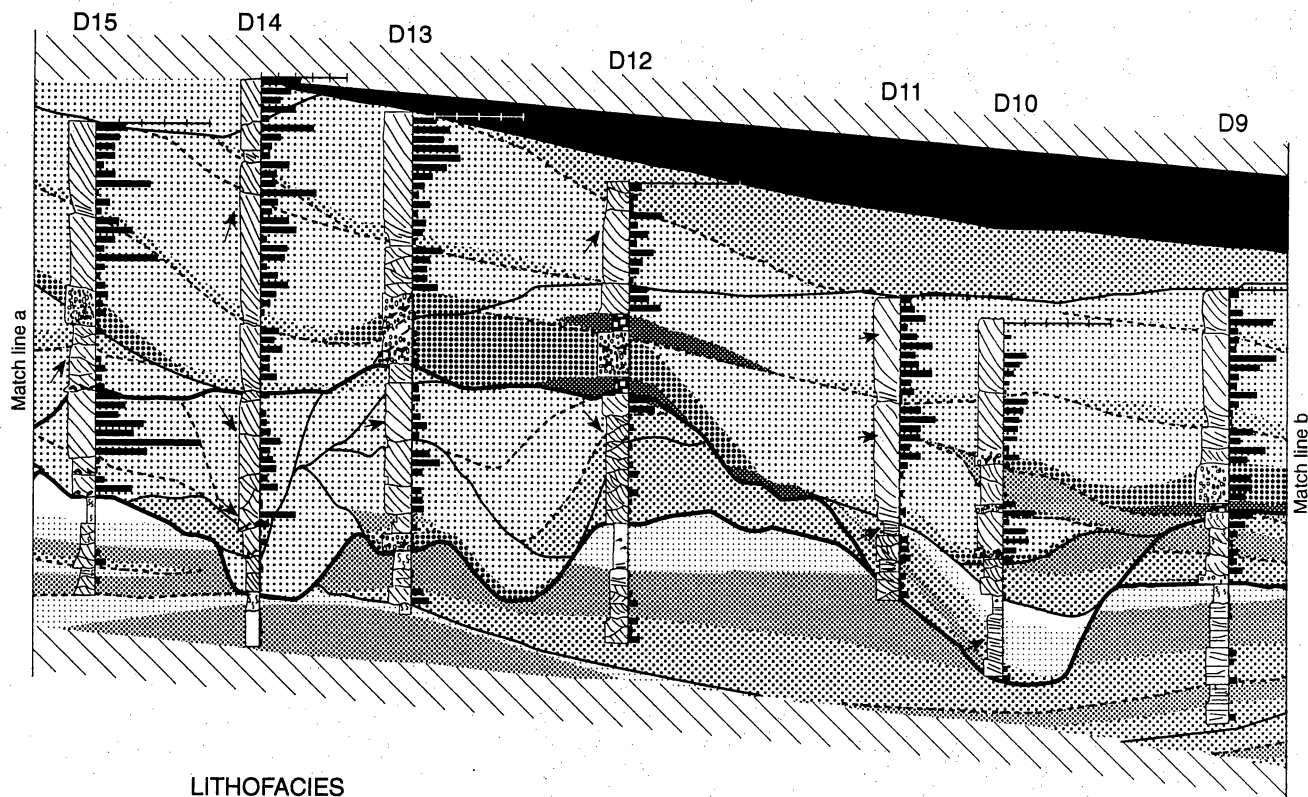
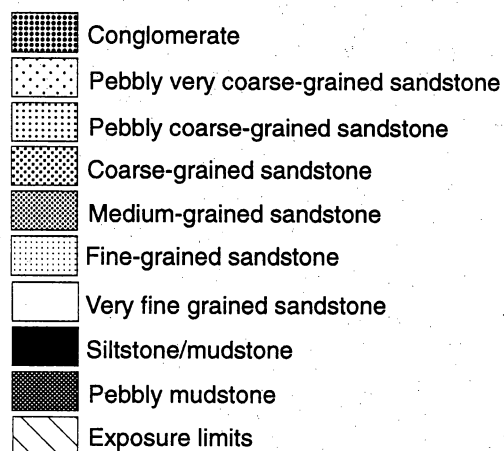


Figure 3c. Cross section showing distribution of permeability profiles and grain size classes, Km 99.



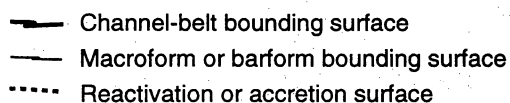
LITHOFACIES



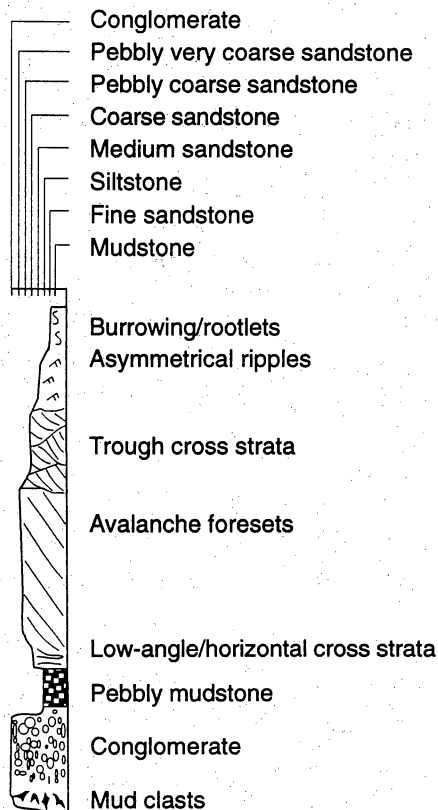
D9 Transect number

→ Paleocurrent direction relative to north

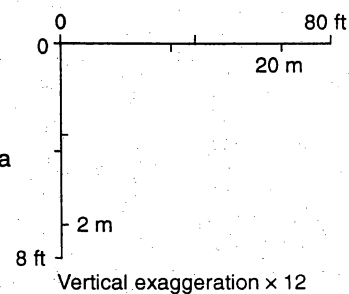
BOUNDING SURFACE HIERARCHY



LITHOLOGIC SECTION



PERMEABILITY PROFILE



QAb354(c)c

Figure 3c (continued)

subarkosic in composition (Becker and others, 1992). Diagenetic cements in order of abundance include calcite, kaolinite, and quartz. Quartz cement, which precipitated early in the diagenetic history, occurs as overgrowths. Calcite postdates quartz cementation and is most abundant along sand/shale contacts. Kaolinite appears to be a weathering product related to the alteration of feldspars. Clay matrix is rare and, when present, is due to infiltration, compaction of clay clasts, or alteration of feldspars (B. Carrasco, personal communication, 1994).

Architecturally, the sandstone body is composed of multiple truncating channel storeys that display vertically stacked and sidelapping relationships. Storeys are defined by a basal erosion surface, which typically displays meter-scale relief, that is overlain by an intraformational mud-clast breccia. Individual storeys range in thickness from 1 to 5 m and extend in length from 20 to 240 m. Component bedsets within channel storeys generally steepen (channel bar) then progressively decrease in dip from the concordant to discordant storey margin (channel fill). Paleocurrents are largely directed northeast to northwest. Sediment disruption in the form of burrowing and root casts causes poor preservation of current structures, especially within the upper portion of channel storeys that are not top truncated. Trace fossils consist largely of simple, unbranched to branched, tube-shaped burrows of various diameters (0.5 to 5.0 cm). Principal zones of sediment disruption separate the sandstone body into three intervals (storey sets) that consist of a basal erosion surface, overlain by a set of channel storeys, and capped by a zone of sediment disruption or burrowing. The three storey sets are designated from oldest to youngest as i, ii, and iii. Individual channel storeys are labeled from oldest to youngest in figure 3a (A through R). Because grain size, sedimentary structures, and paleocurrents vary in a systematic fashion between each storey set, features of each are discussed separately.

Storey set i consists of a pair of truncating channel storeys (A and B) that erosionally overlie the mudstone-dominated and heterolithic fine-grained sandstone facies. The storeys are 3 to 5 m thick and display apparent widths of 100 to 150 m. Paleocurrents are directed north to northwestward. Storey A consists of an upward-fining succession of pebbly, very coarse to medium-grained sandstones. Bedsets are 0.5 to 2 m thick and gently inclined in an upstream

direction. Structures include medium to large trough cross strata and avalanche foreset bedding in which component bedsets climb over the top of underlying bedsets. In contrast, storey B consists of an upward-fining succession of coarse-grained to very fine grained sandstones (fig. 4). Medium-scale trough cross stratification is the dominant sedimentary structure within the lower portion of the succession, whereas planar-parallel stratified sandstones predominate in the mid to upper portions. Near the upstream margin of the storey, small scale rotational slumping, local brecciation, and small-scale soft-sediment deformation are present. Bedsets are concave up to gently inclined (1 to 2 degrees) and onlap the coarser grained channel storey. Bedsets display a flat to gently erosional base and fine upward. Burrowing is common near at the top of each bedset and increases in intensity toward the top of the succession.

Story set ii consists of a series of isolated stories (C, D, and E) that are substantially smaller than those observed in story sets i and iii. Storeys generally range in thickness between 1 and 2 m and display apparent widths of 5 to 60 m. Component bedsets are 0.1 to 0.5 m thick and display apparent lengths of 10 to 45 m. Paleocurrents within this set are directed to the northeast. Individual storeys are composed of a set of gently inclined beds that decrease in thickness and mean grain size upward and in the direction of inclination. Bedsets near the top of the storey are often dominated by parallel, small-scale, cross-laminated or disrupted sandstone, whereas beds lower in the storey are composed of medium-scale trough cross stratification.

Storey set iii consists of a series of highly truncated channel stories (F, G, H, I, J, K, L, M, and N) overlain by a series of well-preserved channel storeys (O, P, Q, and R). The well-preserved channel storeys range in thickness from 3 and 5 m and extend in length 120 to 240 m. The deposition of storeys R and Q followed the deposition of storeys O and P. The deposition of storeys R and Q as well as storeys O and P may have been coeval. Paleocurrents are relatively uniform within a storey but alternate 30 to 45 degrees between adjacent storeys (in a northeast to northwest direction). Biogenic structures are rare and concentrated within the upper 0.1 m of the storey set. Channel storeys consist of three to six bedsets that generally steepen (2 to 4 degree apparent dip) and then progressively decrease in dip from the concordant (channel bar) to



Figure 4. Photograph of transverse bar facies eroding into abandoned channel-fill facies (hand on contact) from section d8.

discordant (channel-fill) channel storey margin. Bedsets downlap an erosional surface that displays meter-scale relief, and they range in thickness from 0.2 to 2 m and are as much as 100 m in length. Channel-bar deposits are characterized by a uniform to upward-coarsening, medium to very coarse grained, pebbly to granular sandstone sequence that passes laterally into channel-fill deposits characterized by a uniform to upward-fining, massive to trough cross-stratified coarse-grained sandstone sequence. Component bedsets also coarsen upward and display large-scale avalanche foreset bedding as thick as 2 m. Foresets dip as much as 33 degrees, are tangential to the underlying surface, and pass laterally into a weakly burrowed, thin-bedded, medium- to coarse-grained, horizontally stratified sandstone or massive pebbly mudstone (fig. 5). Individual foreset laminae consist of a coarse- and fine-grained couplet. Locally, the meter-scale cross stratification may be interrupted by low-angle reactivation surfaces that are capped by a thin veneer of coarse-grained to granular coarse-grained sandstone consisting of small- to medium-scale cross strata. In an upstream direction, where bedsets have not been truncated by the adjacent channel storey, foreset bedding is replaced by medium- to large-scale cross-stratification composed of pebbly, very coarse grained sandstone.

INTERPRETATION OF DATA

Interpretations and reconstructions of channel morphology follow a procedure detailed by Willis (1993), who examined attributes of fluvial deposits within the Himalayan foredeep.

Deposits exposed at Km 99 are interpreted to record deposition within and adjacent to the migrating channel segments of a river. The mudstone-dominated facies is representative of floodplain deposits. Sediments were deposited from suspension by overbank flows during channel flood events. Burrowing, root casts, and carbonate formation record establishment of vegetation between flood events. The thin-bedded, fine-grained, heterolithic facies is interpreted as levee deposits that formed adjacent to the river channel. Individual bedsets were deposited by sheet flows generated by flood events in the main river channel. Complete preservation of small dune bedforms with internal planar cross stratification indicates that sheet flow was capable of

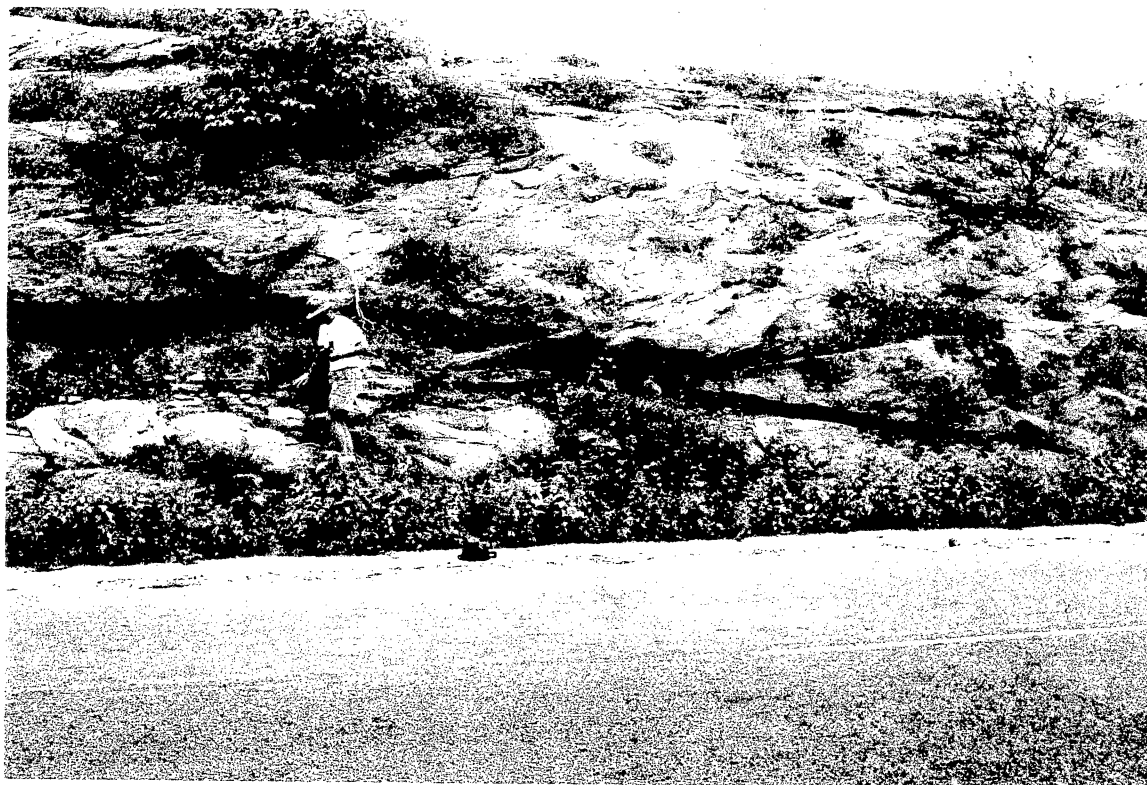


Figure 5. Photograph of transverse bar facies from section d18.

generating dune bedforms. Interbedded mudstones and siltstones capping bedsets suggest deposition from waning currents as the flood subsided. Burrowed intervals formed between flood events as channel margins were vegetated. The sandstone-dominated facies records deposition within a migrating channel in which each storey represents a channel-bar and adjacent channel-fill deposit. Rooted or burrowed zones that vertically separate sets of channel storeys record hiatuses in deposition following channel abandonment or migration. Vertical stacking of storeys sets suggest superposition of channel belts that were present on the floodplain at separate times. Alongstrike stacking of storeys within sets reflects movement of bars and channels within the river associated with channel migration, switching, and cutoff. Bedsets within storeys are composed of sediment accreted during individual flood events. Bedset thickness records the distance that the bar and channel migrated during an individual depositional event. Interpreted channel belt evolution and a plane view of the facies architecture for each storey set are discussed below and illustrated in figures 6 and 7.

Storey set i records the erosion and preservation of a channel-bar and abandoned channel-fill deposits across previously formed floodplain and levee deposits (figs. 6a and 7a). The coarse grain size and upstream accreting bedsets within storey A suggest it represents the upstream portion of a channel-bar deposit. Deposits of storey B are interpreted to represent a channel segment that was undergoing abandonment. The concave-up bedsets, relatively fine grain size, upward-fining trend, abundance of planar-parallel lamination, and high degree of burrowing suggest that the sediments were deposited from waning currents between normally tranquil conditions as channel depth and flow velocities were gradually decreasing. The upstream portion of the channel-bar is the least likely to be preserved because of downstream channel-bar migration.

Storey set ii is interpreted to represent deposits of minor tributaries, or floodbasin drainage channels (figs. 6b and 7a). Storey dimensions indicate channels were smaller than in storey sets i and iii, with depths on the order of 1 to 2 m and widths of 10 to 30 m. The northeast-directed paleocurrent suggests that these channels were flowing toward or away from the main trunk stream. Thin bedsets, medium to coarse grain size, and abundance of planar-parallel and small-

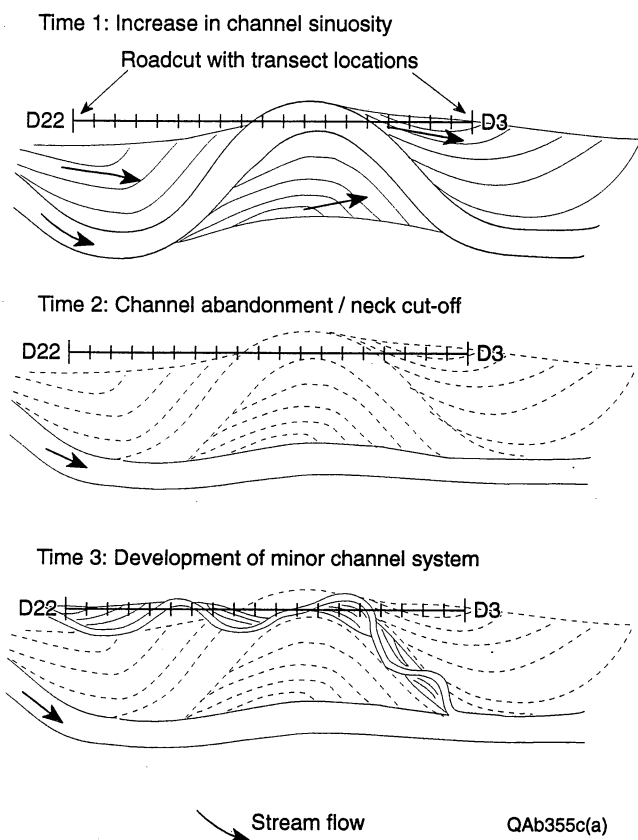


Figure 6a. Channel-belt evolution of storey sets i and ii.

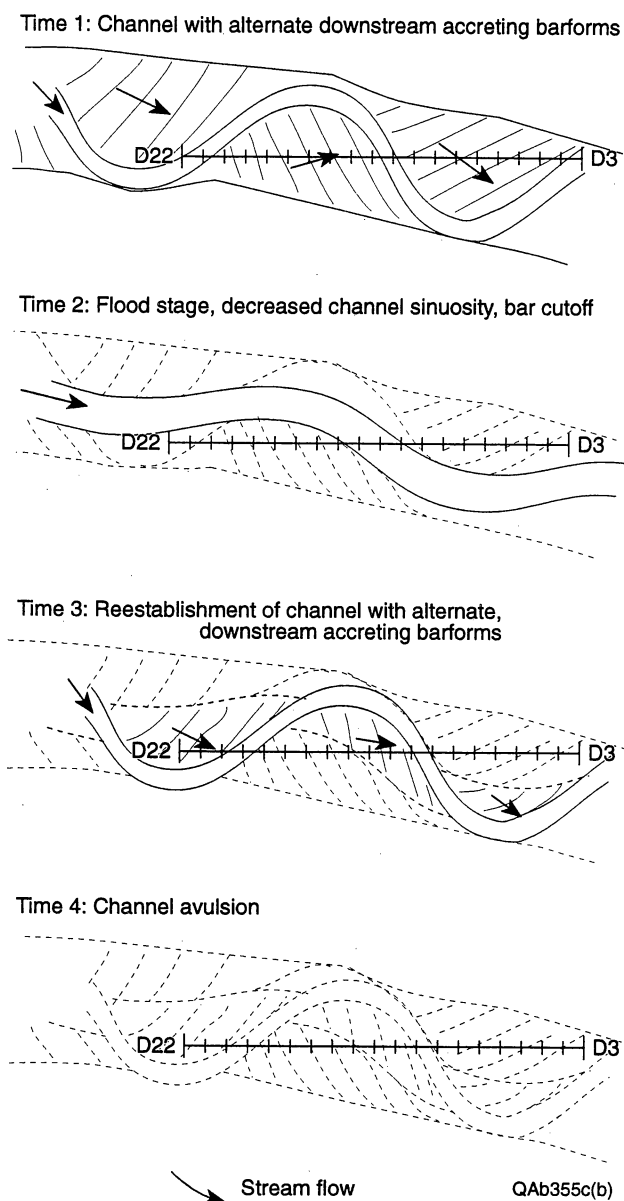


Figure 6b. Channel-belt evolution of storey set iii.

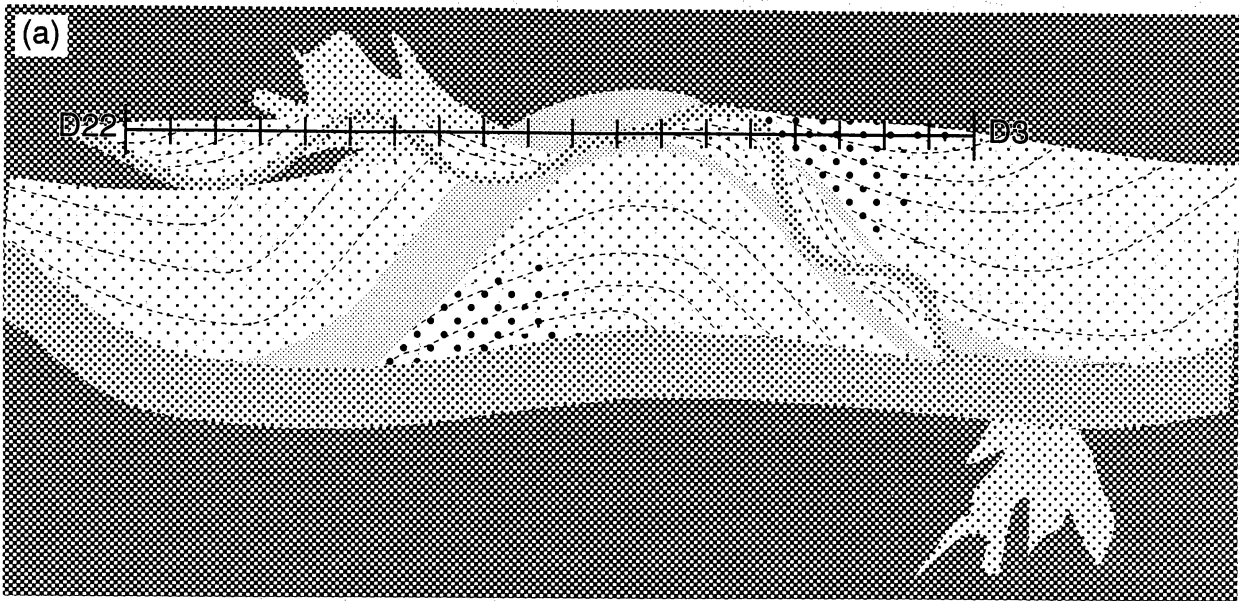
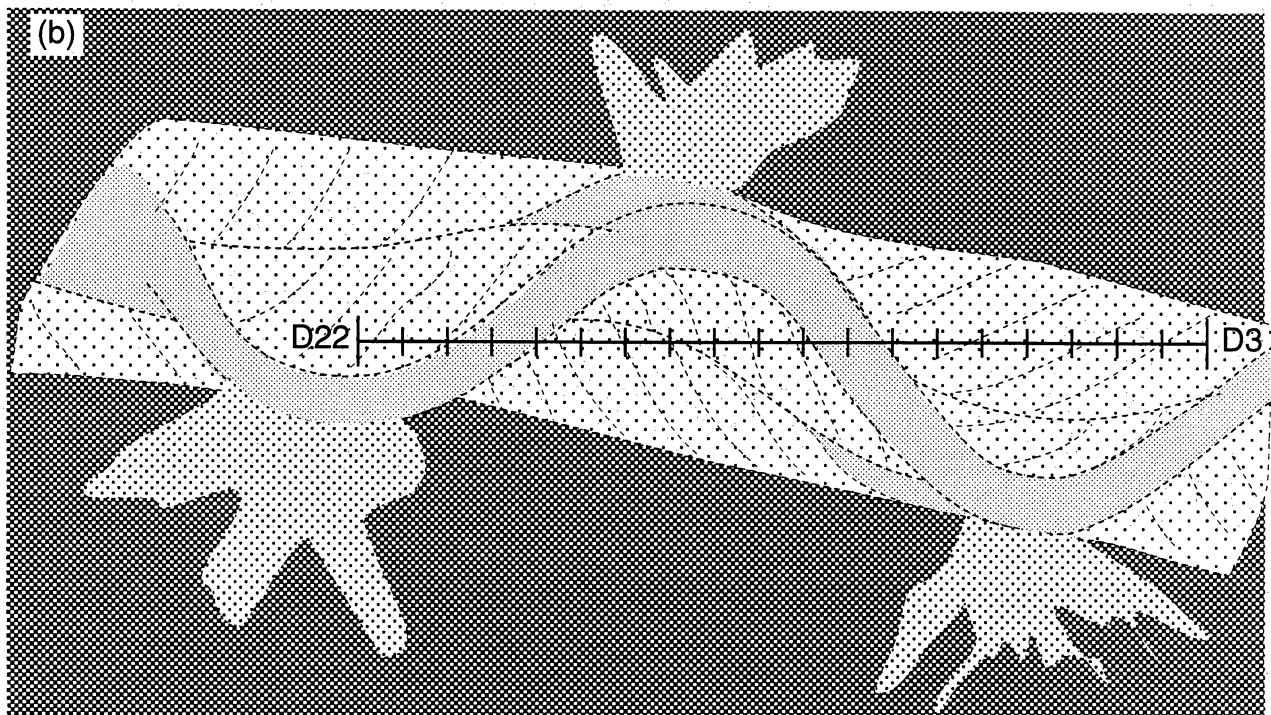



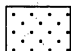
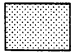



Figure 7a. Plane view of facies architecture for storey sets i and ii.



Lithology

	Mudstone and siltstone		Coarse to pebbly coarse-grained sandstone
	Mudstone, siltstone, fine-grained sandstone		Pebbly, coarse-grained sandstone
	Fine- to coarse-grained sandstone		Pebbly, very coarse grained sandstone

QAb356c

Figure 7b. Plane view of facies architecture for storey set iii.

scale cross stratification suggest generally slower flows and lower deposition rates than in the main channel systems. However, the lack of mudstone-dominated fills suggests that the channels acted as conduits for flood waters until they were completely filled. Pervasive sediment disruption within many of the bodies suggests that much of the channel body was emergent and vegetated between flood events. The single storey nature of the deposits suggests that channels were relatively short-lived or stabilized by vegetation and did not migrate a significant distance. Channels may have acted as conduits for flood waters that overflowed from the main channel system. Position of the drainage channels may have been controlled by areas of low topographic relief associated with finer grained abandoned channel fills of the main trunk stream (Smith and others, 1989).

Storey set iii is interpreted to record the superposition of a series of alternate bars by downstream rather than lateral channel migration within a low- to moderate-sinuosity channel (figs. 6c and 7b). Paleocurrent variations between adjacent truncating storeys suggest that the bars were deposited on opposite sides of the channel. The high preservation of channel-fill deposits truncating downstream dipping-bedsets of the channel bar deposits (see truncation of storey O by R and P by Q in figure 3a) suggests bar superposition by downstream rather than lateral channel migration. The truncation of storey O by Q suggests adjacent bar superposition by channel switching or cutoff. Alternatively, this bedding truncation may record the migration of a single bar that changed shape between two successive depositional events. The relatively high proportion of channel-fill to channel-bar deposits and relatively small number of bedsets (3 to 6) within each channel storey suggest that the channel was not highly sinuous. Because channel-filling deposits are generally concordant and nearly as coarse as bar deposits, the ends of the abandoned channel segments probably did not become rapidly plugged with sediment prior to the channels being filled. Instead, filling of the channels must have been associated with a very gradual diversion of discharge into an adjacent, contemporaneous channel.

Primary stratification within a bedset of the coarse-grained channel bar deposit is very similar in character to a transverse bar deposit described by Crowley (1983) in the upper South Platte River, Colorado. In its simplest form the transverse bar deposits described by Crowley are

composed of three units, apron, foreset, and topset, with each unit resulting from different modes of sedimentation on the lee side, slipface, and stoss side of a transverse bar, respectively. Foreset laminae are formed by avalanching of sediments transported to the slipface by smaller bedforms such as dunes. As these bedforms add sediment to the barform slipface, the coarser particles avalanche down the slipface before the finer particles, yielding coarse-grained and fine-grained couplets. The coarse-grained sediments are usually trapped on the upper to middle sections of the slipface slope; the finer sediments are distributed evenly over the slipface by grain avalanching and grain fall. The apron laminae are formed by deposition of grain-fall sediments taken into suspension from the stoss side of the barform. Coarser sediments fall out of suspension directly downstream from the slipface, whereas finer grained sediments settle out of suspension farther downstream. The apron unit consists of horizontally laminated and ripple-cross-stratified sandstones as well as pebbly mudstones. Topset beds record the movement of dunes and sand waves up the stoss side of the bar. Topset beds are the least likely unit to be preserved because they form on the top and upstream portion of the bar deposit, which is the most susceptible to erosion by the upstream barform. Low-angle truncating surfaces that separate the meter-scale avalanche foreset bedding within bedsets reflect reworking of the bar top by falling-stage flows. The uniform to upward-coarsening grain size trend, bedset dip, and paleocurrent directions suggest that the transverse bars were accreting in a downstream direction.

PERMEABILITY CHARACTERISTICS AND STRUCTURE

This part of the investigation was aimed at identifying which physical attributes of the rocks influence permeability and at quantifying that relationship. The basic idea was to find classifications of the data that minimize variations within classes and maximize differences between classes. To make a study such as this as useful as possible, it is desirable that the classification scheme be relatively simple, based on attributes that are portable to the subsurface, and that the spatial distribution of properties be statistically homogeneous and easily described. During the description process it became apparent that grain size is the dominant control on permeability.

Other factors that may be of secondary importance are sorting, the presence of ductile mudclasts, and preferential calcite cementation. Because of the obvious qualitative relationship of permeability to grain size, we concentrated on classification by grain size. If the effect of grain size were not so obvious, a multivariate analysis would have been employed. The arithmetic, geometric, and harmonic means for each group are presented in table 1. The arithmetic and harmonic means represent upper and lower limits, respectively, on possible effective horizontal and vertical permeabilities. The geometric mean represents a good estimate of the effective permeability when there is no preferred direction of spatial correlation (Begg and others, 1986).

Table 1. Permeability characteristics of sandstone body architectural elements, grain size classes, and horizontal transects.

Class	N	Arith. mean (md)	Coeff. of var.	Geometric mean (md)	Coeff. of var.	Harmonic mean (md)	Min. (md)	Max (md)	P-normal dist.
Mud/silt	18	0.1	-	0.1	-	0.1	0.1	0.1	-
Fine sandstone	57	19	1.1	5.4	1.26	0.58	0.1	110	0.29
Medium ss	97	55	0.71	18	0.75	0.99	0.1	343	0.30
Coarse ss	186	143	0.82	73	0.25	42.2	2	667	0.20
Pebbly coarse ss	391	404	0.97	278	0.18	34.4	0.1	2026	0.32
Pebbly very coarse ss	90	679	1.23	522	0.13	331	34	2194	0.32
Conglomerate	27	166	1.1	88	0.29	32.8	0.5	828	0.22
Levee	48	45	1.78	8	1.26	0.5	0.1	510	-
Abandoned channel fill	55	54	1.31	16.4	0.74	1.1	0.1	327	-
Channel fill	225	167	1.32	59	0.5	2	0.1	1817	-
Channel bar	580	395	0.93	217	0.38	4.8	0.1	2194	-
Total	1417	315	1.16	115	0.43	2.4	0.1	2194	0.31
Horizontal transect: total	505	345	1.14	129	0.41	2.8	0.1	2061	0.31
Horizontal transect: 1 m	315	335	1.24	95	0.51	1.75	0.1	2026	0.29
det 2 (ab) ¹	71	110	0.71	523	0.1	49	5.4	485	0.40
det 1 (cf) ²	61	305	0.72	83	0.2	150	30.6	887	0.34
det 3 (cb) ³	79	628	0.6	115	0.43	422	176	2061	0.24

¹Horizontal transect: medium-grained, planar-laminated sandstone

²Horizontal transect: coarse-grained, trough cross-stratified sandstone

³Horizontal transect: pebbly, coarse-grained, trough cross-stratified sandstone

A probability plot of permeability for grain size classes is shown in figure 8. The seven grain-sized based groups formed six facies-related permeability groups. Predictably, there is a consistent trend of increasing permeability with increasing grain size, demonstrating that grain size is a major control on permeability. From highest to lowest permeability, pebbly very coarse grained sandstones averaged 679 md, pebbly coarse grained sandstones averaged 391 md, coarse-grained sandstones averaged 186 md, medium-grained sandstones averaged 97 md, and fine-grained sandstones averaged 5.4 md. The coarsest grain-size class, conglomerate, displayed permeabilities that were similar to the coarse-grained sandstone, averaging 166 md. The lower than expected permeabilities within this class are attributed to the relatively higher proportion of intraformational clay clasts. During compaction ductile clay clasts are deformed into pseudomatrix, thus reducing the amount of primary porosity. Because most of the permeability measurements collected from the siltstones and mudstone groups were below detection limit of the MFP (>0.09 md), they formed a single low-permeability group. Within each class, permeabilities varied between 2 and 3 orders of magnitude. The coefficient of variations range from 0.71 to 1.23. The observed coefficient of variations are higher than documented for similar classes in distributary-channel and valley-fill deposits, which generally ranged from 0.25 to 0.8.

The fact that permeability is related to grain size suggests a correlative relationship between gamma-ray response and permeability. Gamma-ray responses from Açu Formation wells show that major bounding elements between architectural elements reveal high gamma-ray counts and a general correlation between gamma-ray response and grain size. Nolla (1992) identified three electric log facies that corresponded lithologically to siltstone- and mudstone-dominated successions, very fine to medium-grained sandstones and conglomerates containing abundant mudclasts, and medium- to very coarse grained sandstones and conglomerates.

Permeability Characteristics

A comparison of permeability characteristics for each stratal element is shown in figure 9. Predictably, stratal elements that contain a high proportion of coarse-grained lithologies display the

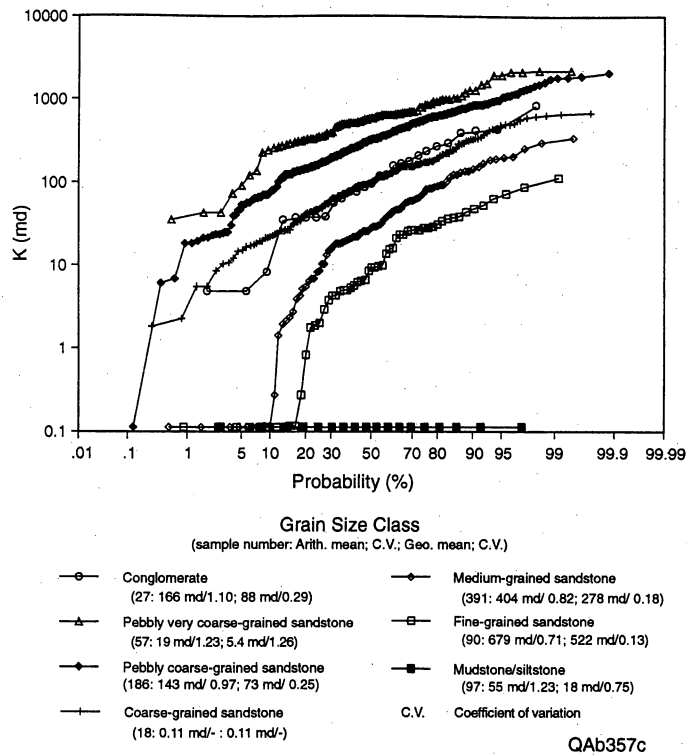


Figure 8. Probability plot of permeability versus grain size.

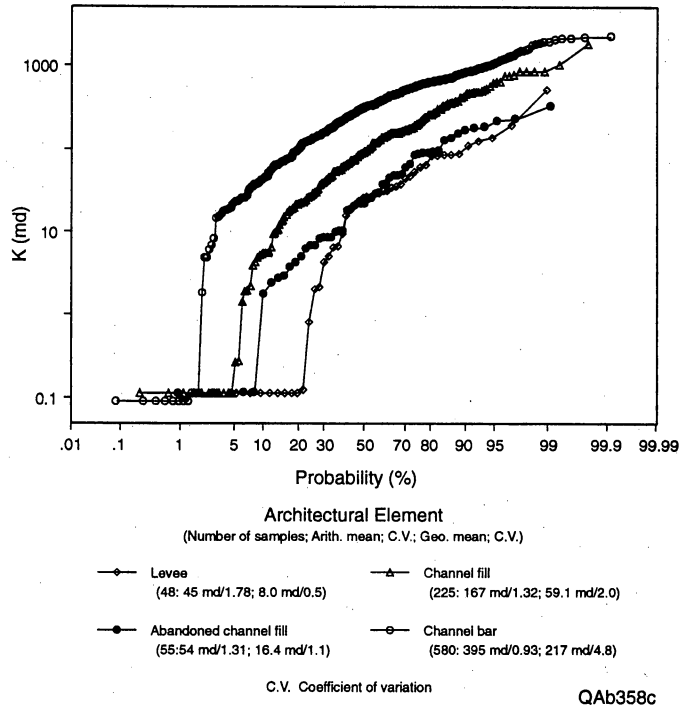


Figure 9. Probability plot of permeability for architectural elements.

highest permeabilities, whereas stratal elements that contain a high proportion of fine-grained lithologies display the lowest permeabilities. Permeabilities are more variable than within the grain-size based groups, typically ranging between 3 and 5 orders of magnitude. The greater variability is indicated by the higher coefficient of variation, which averages 0.74 compared to 0.47 for the grain-size-based groups. The highest permeabilities were observed within the channel-bar facies, which averaged 217 md. Permeabilities ranged from less than 0.1 md to more than 2,000 md. The channel-fill facies displayed intermediate permeabilities, averaging 59 md. Permeabilities ranged from less than 0.1 md to more than 1800 md. The abandoned-channel-fill and levee deposits displayed the lowest permeabilities, averaging 16 and 8 md, respectively. Within each of these groups permeability ranged from less than 0.1 to more than 300 md. The value of identifying permeability characteristics for each stratal element is that the uncertainty associated with simulating the spatial distribution of permeability in analogous reservoirs can be reduced by identifying component architectural elements from vertical successions or well log characteristics.

Permeability Structure

Visual comparison of permeability profiles (fig. 3c) was used to assess whether predictable permeability trends exist within stratal elements. Based on permeability profiles, vertical permeability trends were classified as decreasing upward, increasing upward, uniform, or erratic (no clear trend) (Dreyer and others, 1990). A visual comparison of permeability profiles and stratal architecture indicates the following patterns: (1) permeabilities are reduced one to three orders of magnitude near bedset and channel-storey bounding surfaces; (2) channel-bar deposits and component bedsets are characterized by consistent upward-increasing permeability trends; and (3) channel-fill deposits are characterized by reduced permeabilities that display an erratic to upward-decreasing trend.

Permeabilities near bedset and storey bounding surfaces were reduced between one and three orders of magnitude compared with sandstones 0.2 to 0.5 m above this surface. Reduced permeabilities near storey bounding surfaces are caused by the presence of (1) sandstones

containing abundant intraformational clay clasts, which during burial and compaction have been deformed into pseudomatrix, and (2) pebbly mudstones present as thin discontinuous lenses within deeply scoured portions of the channel bed. Mudclast-rich sandstones and conglomerates were deposited as a widespread but discontinuous channel lag that ranges in thickness between 0.1 and 0.5 m. Reduced permeabilities near bedset bounding surfaces reflect superposition of pebbly coarse-grained avalanche foreset beds deposited along the bar slip face over the top of pebbly mudstones or medium- to coarse-grained apron deposits at the base of the bar.

Individual bedsets containing avalanche foreset bedding typically display an upward-increasing permeability trend. This trend may reflect decreases in grain size and sorting that occur down the slipface of an avalanche foreset bed and that have been documented by Crowley (1983) within transverse bars on the South Platte River. Distinctive changes in grain size and sorting were not noted within avalanche foreset bedding of the Açu outcrop, but such trends are possible. Although the majority of permeability models for channel sand bodies have been based on the classical upward-fining point-bar model, which predicts permeability to decrease from the base up, most Açu channel-bar deposits display an erratic but upward-increasing permeability trend. Dreyer and others (1990) related the lack of an upward-decreasing permeability trend within distributary channel sandstone bodies to increased sorting and winnowing of fines caused by conditions of vertical aggradation (shallowing) and a generally constant high discharge in the channel. Laterally accreting channel-bars, levees, and channel-fills in the Açu Formation typically display an upward-decreasing permeability trend. The upward-fining grain size trends reflect deposition from waning flows that decrease in velocity as the channel is gradually abandoned. In a lateral direction, channel storeys typically display an overall decrease in permeability from the upstream portion of the channel bar to the channel fill. In general, permeability decreases from 500 to 2,000 md within the pebbly very coarse grained channel bar to 50 to 500 md within the medium- to coarse-grained channel fill.

Large-scale permeability trends reflect processes associated with bar growth, channel migration or bar movement, and bar preservation. Permeability trends may be disrupted where

channel storeys are truncated and poorly preserved. Channel storeys are best preserved along the margins and upper portion of a channel belt and poorly preserved near the central and lower portion of the channel belt. The proportion of channel-bar to channel-fill deposits may be altered by changes in channel sinuosity. High-sinuosity channels are dominated by lateral channel migration and preserve a greater proportion of the channel bar than low sinuosity channels, in which downstream migration dominates over lateral migration. Finally, permeability trends may be composed of multiple upward decreasing or increasing trends due to vertical superposition of different channel belts.

Spatial Correlation of Permeability

The semivariogram technique was used to investigate the lateral and vertical correlation of permeability within different lithofacies and large-scale stratal elements. The technique was applied on data sets in which permeability was collected at a spacing of 0.1 m over a distance of approximately 6 to 7 m. Permeability data were collected within (1) a bed of large-scale, cross-stratified, pebbly coarse-grained sandstone parallel to paleocurrent, (2) a bed of large-scale, cross-stratified, coarse-grained sandstone normal to paleocurrent, and (3) a bed of horizontally stratified medium-grained sandstone. The experimental semivariogram for each data set is shown in figure 10. For all three data sets the experimental semivariogram displayed a relatively high degree of variation with little or no range of influence (the distance from the origin to where the curve levels off). These characteristics indicate that at distances greater than 0.1 m (sample spacing) and less than 3 to 4 m (half the transect length) permeability within bedsets composed of similar grain sizes is uncorrelated or distributed in a largely random fashion. Orientation of the data set relative to paleocurrent direction (parallel versus normal) does not appear to influence the spatial continuity of permeability.

The technique was also applied on a data set in which permeability was collected in a horizontal fashion at spacing of 1 m over a distance of 325 m within the sandstone body. The experimental vertical and horizontal semivariograms for the sandstone body are shown in

figure 11. At a larger scale, the data show a much different correlation structure. The semivariogram function continues to increase and is correlated over the range investigated, a distance of several hundred meters laterally. In addition, the vertical correlation structure is very similar to the horizontal correlation structure, differing only in scale, with the horizontal correlation range greater than the vertical by a factor of about 50. The correlation structure suggests that the data may be distributed in a fractal manner. The correlation structure may be explainable in terms of the magnitude or degree of variation that exists between bedsets and channel storeys. If this is the case, the ratio of the vertical and lateral dimensions of bedsets and channel storeys should also be about 50:1. This in fact is the case. Bedset thicknesses are between 0.5 and 2 m and range in length between 50 and 100 m. Channel storeys range in thickness from 3 to 5 m and in length between 100 and 250 m. Results from this analysis suggest that the horizontal correlation range may be predictable from vertical well data, in which storey thickness, bedset thickness, bedset inclination and direction of dip, and the vertical fractal dimension can be determined, and from outcrop information in which estimates of channel sinuosity and storey preservation can be obtained.

STRATAMODEL GEOCELLULAR PERMEABILITY MODEL

A two-dimensional representation of permeability structure for the reservoir analog was constructed using Stratamodel Stratigraphic Geocellular Modeling software (SGM). The SGM technique preserves geologic reality by using lithologic and stratigraphic information to deterministically interpolate permeability values.

Work on the model began after information gathered on the outcrop had been assembled into a cross section depicting bedding architecture, distribution of principal lithofacies, and measured permeability values for each vertical transect. The procedure for building a 2-D model of permeability includes (1) preparing a data base of geologic and petrophysical attributes for input into Stratamodel, (2) constructing a series of 2-D framework grids (sequences), (3) selecting

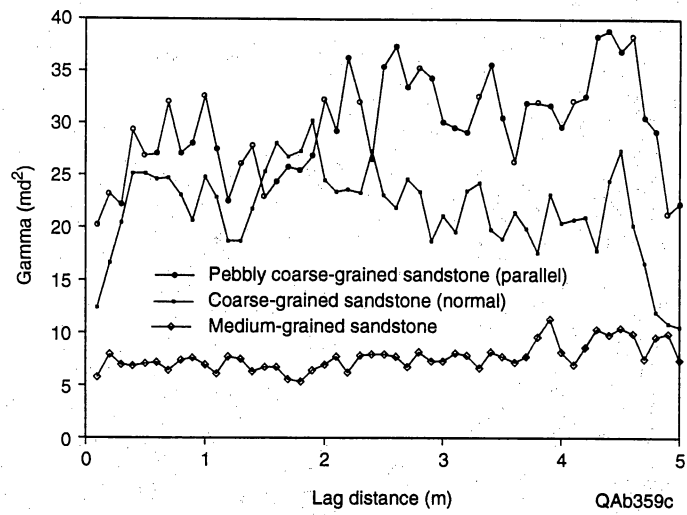


Figure 10. Semivariogram of permeability for pebbly coarse-grained and medium-grained sandstone.

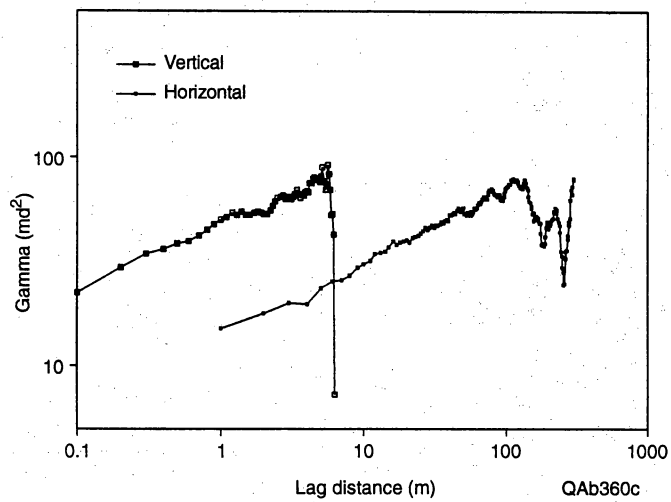


Figure 11. Semivariogram of permeability for erosive-based sandstone body.

appropriate fill patterns and cell thicknesses for each sequence, and (4) interpolating permeability values between transects.

In the first step, a data base was constructed that included measured permeability values, a vertical and horizontal position in meters relative to an arbitrary datum, a permeability measurement in millidarcys, and a list of geologic attributes such as lithology, grain size, sedimentary structures, and interpreted facies.

In the second step, a series of chronostratigraphic 2-D framework grids referred to as sequences were generated. The sequences provide separation of geologic or petrophysical properties. Using the geologic cross section of the outcrop as a template, depositional and lithologic boundaries or surfaces were used to define sequences. The surfaces were input into Stratamodel by digitizing them directly from the geologic cross section. Sequences are created by ordering the surfaces chronostratigraphically or in a depositional time sequence within the Stratamodel program. This process allows scouring or truncating events to be represented. A total of 106 sequences were identified. Sequences are illustrated in the foldout labeled Stratamodel sequences.

In the third step, a fill pattern and cell thickness for each sequence were selected. Fill patterns include onlap, downlap, parallel, and proportional bedding. In general, the fill pattern was selected to match the depositional pattern of the sequence as well as possible. However, the proportional fill pattern was used for sequences that contained too few permeability data. The thickness of individual cells was kept at 0.05 m to avoid averaging permeability values.

The final step involved interpolating permeability values between measured values. Stratamodel does a linear interpolation that is confined by the sequence boundaries and guided by the fill patterns. Because random variation within lithofacies is not accounted for with this procedure, the deterministic realization will display a lower variance than the true variance.

Numerous iterations and modifications of these procedures were performed until a satisfactory realization was achieved. The final SGM permeability model is illustrated in the foldout labeled Stratamodel permeability.

CONCLUSIONS

(1) Açu Formation facies exposed at Km 99 are interpreted to record deposition within and adjacent to the migrating channel segments of a river. The mudstone-dominated facies is representative of floodplain deposits. The thin-bedded, fine-grained, heterolithic facies is interpreted as levee deposits that formed adjacent to the river channel. The sandstone-dominated facies records deposition within a migrating channel.

(2) Within the sandstone-dominated facies rooted or burrowed zones vertically separate sets of channel storeys deposited by different channel belts that were present on the floodplain at separate times. Within each storey set, truncating relationships between adjacent storeys record the superposition of a series of alternate bars within a low- to moderate-sinuosity channel by downstream rather than lateral channel migration. The fact that channel-fill deposits are nearly as coarse as channel-bar deposits indicates that channel segments were not rapidly abandoned; instead, filling must have been associated with a gradual diversion of discharge into an adjacent channel.

(3) Each storey represents a channel-bar and adjacent channel-fill deposit. The arrangement and characteristics of component bedsets indicate that the principal type of channel storey was formed by a series of transverse bars that accreted in a downstream fashion.

(4) Grain size is the dominant control on permeability. Other factors that are of importance are sorting and the presence of ductile mud clasts. Inasmuch as each architectural element displays differences in grain size and bedding architecture, it is not surprising that they display differences in permeability structure.

(5) A visual comparison of permeability profiles and stratal architecture indicates that (1) permeabilities are reduced one to three orders of magnitude near bedset and channel-storey bounding surfaces, (2) channel-bar deposits and component bedsets are characterized by consistent upward-increasing permeability trends, and (3) adjacent channel-fill deposits are characterized by reduced permeabilities that display an erratic to upward-decreasing trend.

(6) The fact that grain size is related to permeability suggests that permeability relationships may be portable to the subsurface setting using conventional well log tools. The amount of uncertainty associated with simulating the spatial distribution of permeability in analogous reservoirs may be reduced if component architectural elements could be identified from vertical successions.

(7) Results from this analysis suggest that the horizontal correlation range and three-dimensional distribution of lithologies may be predictable from vertical well data in which storey thickness, bedset thickness, bedset inclination and direction of dip, and vertical fractal dimension can be determined, and from outcrop information in which estimates or assumptions regarding channel sinuosity and storey preservation can be obtained.

ACKNOWLEDGMENTS

Funding for this research was provided by Petrobras under contract no. 6502032931. Logistical support for fieldwork in Brazil was provided by Petrobras employees Mauro Becker, Cláudio Bettini, Paulo Cordeiro, Alexandre Siqueira, and Cristiano Sombra and BEG employee Shirley P. Dutton. This report was reviewed by Shirley P. Dutton, Richard P. Major, Brian Willis, and Tucker F. Hentz and edited by Amanda R. Masterson. Illustrations were prepared by William C. Bergquist. Word processing and text layout were by Susan Lloyd.

REFERENCES

- Allen, J. R. L., 1963, A review of the origin and characteristic of recent alluvial sediments: *Sedimentology*, v. 5, p. 89–191.
- Becker, M. R., Carrasco, B. N., Junior, A. B. B., Ribeiro, C. A. F., Assis, O. C., Cordeiro de Farias, P. R., and Preda, W., 1992, Projeto Geometrias E Heterogeneidades De Reservatorios Fluvias: Formacao Açú, Bacia Potiguar. CENPES/DEPEX/DEBAR/RPNS, PETROBRAS/ CENPES (Relatorio interno).

- Begg, S. H., Carter, R. R., and Dranfield, P., 1986, Assigning effective values to simulator grid blocks in heterogenous reservoirs: Society of Petroleum Engineers, SPE Paper 16754.
- Carrasco, B. N., 1994, Acompanhamento das Operacoes de Campo com Minipermeametro e Mapeamento do Afloramento do Km 99 da Br-304 Açú-Mossoro. Centro De Pesquisas E Desenvolvimento, PETROBRAS/ CENPES (Relatorio interno), 31 p.
- Castro, J. C., Lima, H. P., and Barrocas, S. L., 1981, Facies, diagenese e modelos de acumulacao da Formacao Açú, parte emersa da Bacia Potiguar, Rio de Janeiro. PETROBRAS/ CENPES (Relatorio interno).
- Cordeiro de Farias, P. R., Carneiro de Castro, J., Tibana, P., and Barrocas, S. L. S., 1990, Cretaceo Da Bacia Potiguar, PETROBRAS/ CENPES (Relatorio interno).
- Crowley, K. D., 1983, Large-scale bed configurations (macroforms), Platte River Basin, Colorado and Nebraska: primary structures and formative processes. Geological Society of America Bulletin, v. 94, p. 117–133.
- Dreyer, T., Scheie, A., and Walderhaug, O., 1990, Minipermeameter-based study of permeability trends in channel sand bodies: American Association of Petroleum Geologist Bulletin, v. 74, no. 4, p. 359–374.
- Friend, P. F., 1983, Towards a field classification of alluvial architecture or sequence, *in* Collinson, J. D., and Lewin, J., eds., Modern and ancient fluvial systems, International Association of Sedimentologists, Special Publication, p. 345–354.
- Goggin, D. J., Thrasher, R. L., and Lake, L. W., 1988, A theoretical and experimental analysis of minipermeameter response including gas-slippage and high velocity flow effects: In Situ, v. 12, p. 79–116.
- Jackson, R. G., II, 1975, Depositional model of point bars in the lower Wabash River: Journal of Sedimentary Geology, v. 46, p. 579–594.
- Jensen, J. L., Lake, L. W., and Hinckley, D. V., 1987, A statistical study of reservoir permeability: distributions, correlations, and averages: Society of Petroleum Engineering Formation Evaluation, December, p. 461–468.
- McBride, E. F., 1963, A classification scheme of common sandstone: Journal of Sedimentary Petrology, v. 33, p. 664–669.

- Miall, A. D., 1985, Architectural-element analysis: a new method of facies analysis applied to fluvial deposits: *Earth-Science Reviews*, v. 22, p. 261–308.
- Miall, A. D., 1988a, Reservoir heterogeneities in fluvial sandstones: lessons from outcrop studies: *American Association of Petroleum Geologists Bulletin*, v. 72, p. 682–697.
- Miall, A. D., 1988b, Architectural elements and bounding surfaces in fluvial deposits: anatomy of the Kayenta Formation (Lower Jurassic), southwest Colorado: *Sedimentary Geology*, v. 55, p. 233–262.
- Nolla, F. R., 1992, Atualizao Do Estudo Do Arenitos Reservatorios Da Unidade 3 Da Formacao Açu-Campo De Alto Do Rodriques-Bacia Potiguar Emersa. DEBAR/DIREX/SELAG, PETROBRAS/ CENPES (Relatorio interno).
- Stalkup, F. I., and Ebanks, W. J., 1986, Permeability variation in a sandstone barrier-tidal channel-tidal delta complex, Ferron Sandstone (lower Cretaceous), central Utah: *Society of Petroleum Engineers*, SPE Paper 15532, 13 p.
- Vasconcelos, E. P., Neto, F. F. L., and Roos, S., 1990, Unidades de correlacao da Formaca Açu—Bacia Potiguar. PETROBRAS/DEPEX/DEBAR (Relatorio interno), 14 p.
- Willis, Brian, 1993, Ancient river systems in the Himalayan foredeep, Chinji Village area, northern Pakistan: *Sedimentary Geology*, v. 88, p. 1–76.